AD-A168 400 CLEAR AIR TURBULENCE ANALYSIS USING ISENTROPIC METHODS 1/2
(U) NAVAL POSTGRADUATE SCHOOL MONTEREY CA J H JACOBSON
MAR 86

UNCLASSIFIED F/G 4/2 NL

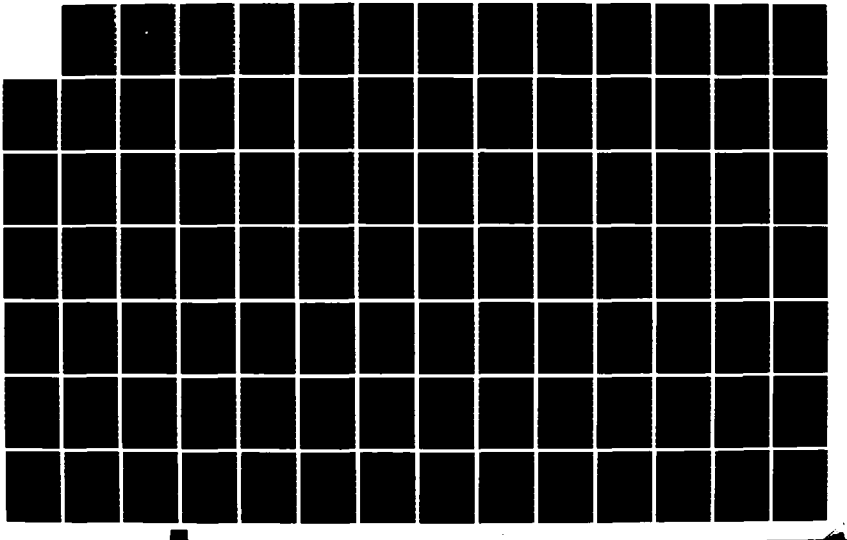

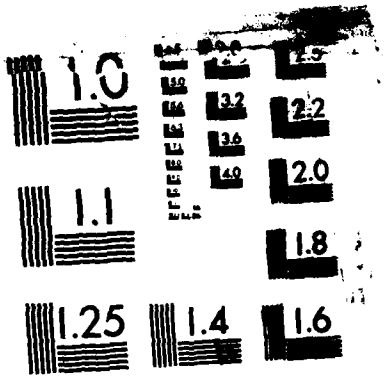

MICROCOPY RESOLUTION TEST CHART
NATIONAL BUREAU OF STANDARDS 1963-A

NAVAL POSTGRADUATE SCHOOL

Monterey, California

THESIS

CLEAR AIR TURBULENCE ANALYSIS USING ISENTROPIC METHODS

by

John H. Jacobson

March 1986

Thesis Advisor: C. H. Wash

Approved for public release; distribution unlimited.

URITY CLASSIFICATION OF THIS PAGE

REPORT DOCUMENTATION PAGE

REPORT SECURITY CLASSIFICATION CLASSIFIED	1b. RESTRICTIVE MARKINGS
SECURITY CLASSIFICATION AUTHORITY	3. DISTRIBUTION / AVAILABILITY OF REPORT Approved for public release; distribution is unlimited.
DECLASSIFICATION / DOWNGRADING SCHEDULE	
ERFORMING ORGANIZATION REPORT NUMBER(S)	5. MONITORING ORGANIZATION REPORT NUMBER(S)
NAME OF PERFORMING ORGANIZATION aval Postgraduate School	6b. OFFICE SYMBOL (If applicable) Code 63
7a. NAME OF MONITORING ORGANIZATION Naval Postgraduate School	
ADDRESS (City, State, and ZIP Code) onterey, California 93943-5000	7b. ADDRESS (City, State, and ZIP Code) Monterey, California 93943-5000
NAME OF FUNDING / SPONSORING ORGANIZATION	8b. OFFICE SYMBOL (If applicable)
9. PROCUREMENT INSTRUMENT IDENTIFICATION NUMBER	
ADDRESS (City, State, and ZIP Code)	10. SOURCE OF FUNDING NUMBERS

PROGRAM ELEMENT NO.	PROJECT NO	TASK NO	WORK UNIT ACCESSION NO.

TITLE (Include Security Classification)
LEAR AIR TURBULENCE ANALYSIS USING ISENTROPIC METHODS

PERSONAL AUTHOR(S)
acobson, John H.

TYPE OF REPORT	13b. TIME COVERED	14. DATE OF REPORT (Year, Month, Day)	15. PAGE COUNT
aster's Thesis	FROM _____ TO _____	1985 March	98

SUPPLEMENTARY NOTATION

COSATI CODES		
FIELD	GROUP	SUB-GROUP

18. SUBJECT TERMS (Continue on reverse if necessary and identify by block number)
clear air turbulence, isentropic analysis, objective analysis

ABSTRACT (Continue on reverse if necessary and identify by block number)

ntropic analyses were completed subjectively and by the Petersen (1986) objective analy- scheme for a 24-h Clear Air Turbulence (CAT) outbreak over the midwest United States. purpose of the study is to determine if areas of high CAT potential could be identified subjective isentropic analyses, and then by the automated analyses produced by the Peter- objective analyses. A background of CAT theory and current CAT forecasting techniques also presented. The synoptic situation indicates the importance of the jet stream st- ture in this case. The study reveals that analyzed areas of low Ri and high wind shear respond very well to reports of CAT. The objective analysis performance is fair overall. shows a distinctive weakness in the analysis of the wind speed, occasionally producing rious wind maxima. Analyses of the mass field, frontal slope and Montgomery stream action, are quite successful.

DISTRIBUTION / AVAILABILITY OF ABSTRACT UNCLASSIFIED/UNLIMITED ☐ SAME AS RPT ☐ DTIC USERS	21. ABSTRACT SECURITY CLASSIFICATION UNCLASSIFIED
NAME OF RESPONSIBLE INDIVIDUAL lyle H. Wash	22b. TELEPHONE (Include Area Code) (408) 646- 2295
	22c. OFFICE SYMBOL Code 63Wx

FORM 1473, 84 MAR 83 APR edition may be used until exhausted
All other editions are obsolete

SECURITY CLASSIFICATION OF THIS PAGE

Approved for public release; distribution is unlimited.

Clear Air Turbulence Analysis Using Isentropic Methods

by

John H. Jacobson
Captain United States Air Force
B.S., North Carolina State University, 1980

Submitted in partial fulfillment of the
requirements for the degree of

MASTER OF SCIENCE IN METEOROLOGY

from the

NAVAL POSTGRADUATE SCHOOL
March 1986

Author: John H. Jacobson
John H. Jacobson

Approved by: Carlyle H. Wash
C.H. Wash, Thesis Advisor

R.J. Renard, Second Reader

R.J. Renard, Chairman,
Department of Meteorology

John N. Dyer,
Dean of Science and Engineering

ABSTRACT

Isentropic analyses were completed subjectively and by the Petersen (1986) objective analysis scheme for a 24-h Clear Air Turbulence (CAT) outbreak over the midwest United States. The purpose of the study is to determine if areas of high CAT potential could be identified by subjective isentropic analyses, and then by the automated analyses produced by the Petersen objective analyses. A background of CAT theory and current CAT forecasting techniques are also presented. The synoptic situation indicates the importance of the jet stream structure in this case. The study reveals that analyzed areas of low Ri and high wind shear correspond very well to reports of CAT. The objective analysis performance is fair overall. It shows a distinctive weakness in the analysis of the wind speed, occasionally producing spurious wind maxima. Analyses of the mass field, frontal slope and Montgomery stream function, are quite successful. (Theses)

TABLE OF CONTENTS

LIST OF TABLES

LIST OF FIGURES

ACKNOWLEDGEMENT

First I would like to thank God who sustains me daily and gives my life purpose. I would like to thank Dr. Carlyle Wash who patiently saw me through this research project and to Raymond Kiesa who donated a lot of time to proofread. I would also like to thank Dr. Ralph Petersen for providing his objective analysis model to use for this study. Thanks also go to Mr. Art Gulliver at AFGWC for sending plots of CAT reports for use with this study. Finally, a very special thanks goes to my wife, Chris, whose prayers and encouragement made it possible for me to make it through this program.

1. INTRODUCTION

The effects of Clear Air Turbulence (CAT) are of critical importance to both civilian and military aviation. On 18 July 1982, United Airlines Flight 95 was severely jolted by turbulence over Wyoming. Twenty-four passengers were injured with four being hospitalized (The Washington Post, 18 July 1982). In 1972, United Airlines estimated that CAT-related losses including delays, route alterations, as well as damage to aircraft, were $23 million annually (Jones, 1972). For the period 1963-1965 the U.S. Department of Commerce estimated the CAT damage to military aircraft was $30 million (Jones, 1972). Clearly, CAT-related damage is of concern to both the civilian and military communities.

CAT analysis and forecasting are still in the early development stages compared to other parameters forecasted by modern weather prediction schemes. Currently numerical models do not satisfactorily analyze or forecast CAT. It must be shown it is possible to analyze CAT numerically with the available data before CAT can be numerically forecast.

The purpose of this thesis is to determine if areas of high CAT potential could be identified by subjective isentropic analyses, and then by the automated Petersen three-dimensional objective analysis routine (Petersen, 1986). Isentropic coordinates are especially suited for CAT

analysis because air flow will follow an isentropic surface in the absence of any diabatic processes. Also, isentropic analyses can resolve upper front and jet streak zones, where CAT typically occurs. Using the model output, the gradient Richardson number (Ri) is computed and then compared to the reports of CAT. The capability for analyzing the structure of the upper troposphere with the Petersen model will be crucial if one is to determine an Ri distribution that is associated with CAT occurrences.

The verifying data for this thesis were obtained from the Air Force Global Weather Center (AFGWC). AFGWC provided CAT reports for 19 to 20 March 1982. This case was chosen because of the 26 reports of CAT that occurred over the Midwest United States. Due to the consistent problem of obtaining numerous timely pilot reports, 26 turbulence reports in an area is significant.

The thesis begins with a definition of CAT, a brief CAT climatology and a discussion of causes for CAT. Chapter 3 will synopsize the current United States techniques for the analysis and forecasting of CAT. Chapter 4 discusses the synoptic pattern for the outbreak period. Chapter 5 will discuss the results of the hand analysis and in Chapter 6, the Petersen objective analysis will be presented. Chapter 7 will compare the hand analyses with those obtained by the objective analysis technique and discuss the results of the

CAT analysis study. Chapter 8 will present the conclusions and suggestions for future research.

II. BACKGROUND

Clear Air Turbulence (CAT) is defined as any turbulence in the free atmosphere not in or adjacent to visible convective activity. The International Civil Aviation Organization (ICAO) developed the world-wide specifications of turbulence categories. The specifications for moderate and severe CAT, as published by the World Meteorological Organization (WMO) (Hopkins, 1977), are:

> Moderate - There may be moderate changes in aircraft attitude and/or altitude, but the aircraft remains in positive control at all times. Usually, small variations in air speed. Changes in accelerometer readings of 0.5 g to 1.0 g at the aircraft's center of gravity. Difficulty in walking. Occupants feel strain against seat belts. Loose objects move about.
>
> Severe - Abrupt changes in aircraft attitude and/or altitude; aircraft may be out of control for short periods. Usually, large variations in airspeed. Changes in accelerometer readings greater than 1.0 g at the aircraft's center of gravity. Occupants are forced violently against seat belts. Loose objects are tossed about.

The WMO conducted a study in 1964-65, collecting data from aircrews around the world (Vinnichenko et al., 1980). These data indicated there is a 50% greater frequency of moderate or greater turbulence at elevations >2000 m than at elevations <1000 m. The analysis of the data collected over Europe and America reveal the frequency of turbulence over continents depends strongly on the nature and the height of the relief.

Table 1 from Vinnichenko et al. (1980) lists data on frequency of CAT of differing intensity for various regions around the world. It shows the maximum frequency of turbulence occurs over Japan. The WMO study also revealed the frequency of turbulence is 30-40% less over water than it is over low terrain and that the maximum frequency of turbulence occurs in the upper troposphere at altitudes of 9-13 km within the zone of 15-45^{0}N. Generally, the probability of encountering CAT increases with altitude and reaches a maximum near the tropopause (Dutton and Panofsky, 1970). CAT also occurs in the stratosphere, but less frequently.

CAT observations come from a number of sources. Unfortunately such data are usually subjective in nature. Vinnichenko et al. (1980) graphically illustrated the subjectivity of reporting CAT. Their study compared turbulence reports by air crews to readings from aircraft accelerometers. For accelerometer readings <0.2 g, 71% of the pilots reported light turbulence, 24% reported moderate turbulence and 5% reported severe turbulence. For acceleration $\geq$0.2, but < 0.5 g, 78% of the pilots reported moderate CAT while 22% reported severe CAT. For accelerations $\geq$0.5 g, 100% of the pilots reported severe turbulence. Considering that the WMO has established that turbulence readings of 0.5 - 1.0 g are to be considered only moderate turbulence, one can see that turbulence reporting can be quite subjective.

Incomplete pilot reports also pose another problem in analyzing pilot reports. Many pilot reports indicate turbulence occurred, but the pilots do not indicate whether the turbulence was associated with visible convective activity. Radar summaries and satellite imagery in the area where the report occurred must then be checked to see if the turbulence is CAT or just turbulence associated with convective activity.

The determination of CAT intensity is further complicated by the dependence of airframe response on both the characteristics of the turbulence as well as the aerodynamic properties of the aircraft (Vinnichenko et al., 1980). The effect of given turbulence decreases with increasing aircraft weight and is also a function of aircraft speed.

The identification of areas of turbulence is limited by the scale of the upper-air observations as compared to the scale of turbulence. Browning (1971) reported the vertical scale of the CAT detected by ground-based radars is 600 m. Keller (1981) reported 500 m is an appropriate vertical scale to resolve most mesoscale shear layers. Vinnichenko et al. (1980) reported approximately 70% of the turbulent zones which affect aircraft have horizontal dimensions of <100 km. They further state that shear-induced CAT normally occurs in thin layers 200 m to 1500 m thick and generally has a duration of 30 minutes to one day. Upper-air observations are at 12-h intervals at stations a few hundred

kilometers apart with vertical data points about every 700 m. Comparing the scale of the data to the scale of CAT, the problem of resolving the phenomena with the current data coverage becomes obvious. Even though CAT occurs on such a small scale, CAT analyses should benefit from the higher vertical resolution available using isentropic analyses of radiosonde data to improve horizontal upper troposphere analyses.

Hopkins (1977) provides a good overview of the causes of CAT. He states, "The generally accepted mechanisms responsible for the creation of turbulence in clear air are standing waves in the lee of a mountain barrier, and strong vertical shear in a statically stable layer." In addition, convective updrafts due to the strong surface heating cause low-level turbulence. This thermal CAT rarely causes any damage and will not be addressed. This section will look at causes of CAT associated with wind shear in a statically stable layer, as well as the causes of mountain-induced CAT.

It is well accepted that CAT associated with strong vertical wind shear in a statically stable layer, results in waves that amplify and break similar to a breaking ocean wave (Keller, 1981). This is Kelvin-Helmholtz instability (KHI). The KHI model seems to be in favorable qualitative and quantitative agreement with observations of unstable shear layers and numerical investigations of turbulent scale

motions (Keller, 1981). Thorpe (1973) reproduced the KHI processes in the laboratory.

The development of KHI is related to the gradient Richardson number (Ri), which is defined as:

$$Ri = \frac{g\partial\Theta}{\Theta\partial Z}/(\frac{\partial V}{\partial Z})^2 \qquad (1)$$

where g is gravity, Θ is the potential temperature, z is geopotential height, and V is the wind speed. The Richardson number is a ratio of the work done against gravitational stability due to negative buoyancy to energy being produced by wind shear and transferred from the mean to the turbulent flow. From observations in the laboratory (Thorpe, 1973), measurements in the atmosphere (Browning, 1971), and from continuing research (Thompson, 1980), the critical Ri for KHI is $\leq 1/4$. When the atmosphere has values less than the critical Ri, then it is, or soon will be, undergoing turbulent motion. In Richardson's original argument, there would be enough energy released to do mixing against gravity if the Ri was <1. However, turbulence does not actually appear until Ri =1/4. Thus 1/4 of the kinetic energy is transferred to potential energy and the remaining 3/4 of the energy is cascaded to small enough scales to be dissipated via molecular viscosity effects (Thompson, 1980).

Another form of the Ri developed by Dutton and Panofsky (1970) relates the Ri to the slope of an internal front. An

internal front is a baroclinic zone which can also be characterized as a statically stable layer that accompanies most extratropical cyclones. Many case studies have shown that CAT tends to be concentrated in internal fronts where the Ri is small (Dutton and Panofsky, 1970). Dutton and Panofsky assume the wind shear is approximated by the horizontal gradient of potential temperature. After making simplifying approximations, the following equation results:

$$Ri = \frac{const}{[S^2(g\partial\theta/\theta\partial Z)]}, \qquad (2)$$

where S is the slope of the internal front. With this form of the Ri, it becomes evident that CAT is most likely to occur in regions of hydrostatic stability, provided that the slope of the internal front is sufficiently large.

It might be surprising that turbulence occurs in these areas of hydrostatic stability rather than in unstable layers. However, it is the high stability in these internal fronts that allows the wind shear to build to extreme values. Dutton and Panofsky (1970) argue that external forces compress a layer, which forces both the isotachs and isentropes together until finally the Ri is small enough for turbulence to begin in that layer. They postulate that as the turbulence causes mixing, the air in the center of the stable layer is thoroughly stirred and very little wind shear is left in the middle. This results in the wind shear being concentrated at the edges of the stable layer. The

strong shear at the edges would provide very rapid feeding of energy to the turbulence near the boundary on the original front. This would explain why CAT tends to be most severe and occurs most often at the edges of the stable layers (Dutton and Panofsky, 1970).

Nearly 50% of severe turbulence reports are caused by lee waves (Hopkins, 1977). Mountain waves are caused when a sufficiently strong wind blows normal to a mountain barrier. The mountain-induced lee waves extend from the lower stratosphere to the ground, and can extend 200 km downstream (Hopkins, 1977). Mountain-wave CAT is most intense within 3000 m of the mountain top and 2000 m on either side of the tropopause (Vinnechenko et al., 1980).

The exact wind conditions necessary for terrain-induced CAT vary with topography. The shape of the ridge and the existence of mountain passes are thought to influence the CAT production capacity of a mountain barrier (Hopkins, 1977). Generally a component normal to the ridge line of 15 m/s is needed to induce CAT. This varies from 10 m/s near Denver, Colorado, to 18 m/s over Japan and the eastern U. S. (Lee et al., 1979).

III. CURRENT CAT ANALYSIS TECHNIQUES

The major U.S. agencies issuing CAT forecasts are the U.S. Air Force, the U.S. Navy and the National Weather Service. These agencies agree that CAT occurs at a scale that is too small for their models to resolve accurately. The Air Force and the National Weather Service both use a combined manual and computer method in issuing CAT forecasts, while the Navy makes their CAT forecasts by automated methods. This chapter describes how the different agencies forecast CAT and some of the limitations in their techniques.

A. U.S. AIR FORCE TECHNIQUES

The Air Force Global Weather Central (AFGWC) uses a man-machine approach in forecasting CAT. Their analysis includes monitoring CAT reports, a detailed analysis of the temperature and wind structure of the atmosphere, an analyses of satellite imagery as well as guidance from a computer analysis of CAT potential. As AFGWC receives turbulence reports, their forecasters verify whether the turbulence was CAT or just the turbulence always associated with convective showers/thunderstorms. Personnel that transmit pilot reports could be of great assistance if they would include a remark in the pilot report as to whether the turbulence was

associated with convective activity or not. This would make the verification of CAT reports relatively simple.

CAT reports are monitored to ensure that turbulence is not occurring in areas where it is not currently forecast. The CAT reports are especially helpful to indicate a system which developed and was not forecast to do so. Since some aircraft operations are especially sensitive to turbulence (i.e. air refueling) the forecast needs to be amended. The reports could also indicate the need to cancel a turbulence forecast in an area where many aircraft have flown and not encountered turbulence. Attention is also paid to the fact that turbulence affects different aircraft in different ways. Certainly, the dynamics causing a Cessna pilot to lose control and report severe turbulence would not cause the pilot of a C5-A Galaxie to report severe turbulence.

Upper-air analyses are used to identify areas of turbulence potential. Computer and hand-analyzed charts are inspected to determine the position of the upper-level jet streaks and their relative position with respect to upper-level troughs, ridges and vorticity maxima. Model relationships between positions of jet streaks and synoptic features have proven to be most useful for identifying areas of high CAT potential. For a complete description of these model relationships, see Lee et al., (1979) or Hopkins (1977). The forecasters also check thermal advection patterns since they enhance or decrease the likelihood of CAT. Satellite

imagery is used to aid in locating jet streaks and jet features, especially over data-sparse areas. The forecaster also uses a CAT intensity program (CATI) which analyzes areas of potential turbulence based on an empirical relationship between wind shear and turbulence reports. The empirical relationship, developed at AFGWC, considers the wind shear in a layer as well as the speed. The analysis is based on radiosonde reports and it does not try to spread the data over areas where no radiosonde reports are available. CATI is an analysis program and does not forecast CAT.

After considering the recent reports of CAT, the information obtained from the detailed analysis of the upper-air structure, the empirical relationships of the position of jet streaks to the occurrence of CAT, and the guidance provided by the CATI program, the forecaster then delineates areas where CAT potential is high and forecasts the movement of such areas during the time period. To forecast CAT, the AFGWC forecaster tries to relate the high CAT potential to synoptic features. For example, if a strong jet streak corresponds to an area of high CAT potential, the forecaster models the CAT forecast based on the forecast position of the jet streak. The forecaster also looks at forecast positions of jet streaks to evaluate whether any model relationships conducive to CAT will develop. The Air Force does not have any objective programs that forecast CAT.

Although the AFGWC system is meteorologically sound, there are weaknesses in its approach. Lee et al. (1979) state that "over-forecasting in size and intensity is a common failure of CAT forecasters. At times CAT forecasters 'chase' pilot reports and issue large area CAT advisories just to cover the reports and to protect themselves from any repercussions should an aircraft file a hazard report." Since CAT forecasting relies so heavily on model relationships, the experience level of a forecaster directly influences his ability to accurately forecast CAT. Due to the frequent transfer of military personnel, it is difficult to maintain an experienced CAT forecasting staff. The CATI program is somewhat weak in that it only makes analyses at radiosonde stations. If the baroclinic zone associated with the formation of CAT lies between reporting stations, then the high CAT-potential areas would not be detected.

B. NATIONAL WEATHER SERVICE TECHNIQUES

The National Weather Service (NWS) approach to CAT forecasting appears quite similar to the AFGWC approach. Just as in the Air Force method, they use upper-air analyses, thermal fields, vorticity analyses, satellite imagery and radiosonde reports to determine areas of potential CAT. CAT forecasts are then produced by relating all analyzed and forecast fields to model relationships (National Weather Service, 1979).

C. U.S. NAVY TECHNIQUES

The U.S. Navy Fleet Numerical Oceanography Center (FNOC) produces automated CAT forecasts using a program (CCAT) to delineate areas of CAT. CCAT is computed as a function of the horizontal advection of vertical lapse rate

$$CCAT = \hbar g/fT[\vec{V} \cdot \nabla \partial T/\partial Z] \qquad (3)$$

where $\hbar$ is absolute vorticity, f is the earth's vorticity, g is the acceleration of gravity and $\vec{V} \cdot \nabla \partial T/\partial Z$ is the horizontal advection of the vertical lapse rate. The value of CCAT is directly related forecast turbulence intensity. The values of CCAT range from 0-200, which are associated with turbulence categories of light (0-50), moderate (50-100) and severe (> 100). The Navy low-level turbulence model considers Ri in making low-level turbulence forecasts.

The Navy program has many difficulties. The U.S. Naval Weather Service Products Manual (1976) reports "The various CAT forecasting methods all produce rather disappointing results. Skill scores run about 15-20% on all methods. The CAT program is limited in efficiency and held back from any dramatic improvements. . . ." Furthermore, one of the biggest problems with the CCAT method is the basic premise that "the highest consistent correlation with CAT occurrence was with strong vertical wind shear and vertical instability" (U.S. Naval Weather Service, 1976). This seems to contradict the discussion by Dutton and Panofsky (1970) in Section II. Despite this apparent contradiction, the FNOC method did

show some skill. This is probably because of the large horizontal advection of the lapse rate in the same area as the sloping stable baroclinic zone. Due to the small scale of CAT, it can not be resolved by the FNOC nine-layer Navy Operational Global Atmospheric Prediction System (NOGAPS). This may account for the poor forecasting ability of this scheme.

IV. SYNOPTIC SITUATION

Since model relationships are important in CAT analysis and forecasting, it is important to first examine the synoptic situation for the CAT outbreak dicussed here. The time period of the analyses is for 0000 GMT 19 March 82 to 0000 GMT 20 March 1982. The major factor in the CAT outbreak was the existence of three jet streaks, with wind speeds up to 90 m/s, embedded in two jet stream axes. This chapter will describe the upper-air pattern, the important jet streaks and the surface synoptic situation. Figs. 1-3 and 23-36 are produced by the Petersen objective analysis routine. The 500 mb height and 12-h height change analyses (Figs. 1-3) are used to describe the evolution of the 500 mb pattern. Details from the Petersen analysis scheme are presented in Chapter VI. Figs. 5-19 describe the jet streak pattern. They are subjective isentropic analyses that were drawn from plotted radiosonde data. These analyses were made for 315-335K at intervals of 5K.

A. 500MB PATTERN

An upper low, which moved into the Midwest, is the major feature in the upper troposphere in this case. At 0000 GMT 19 March, the leading edge of the low, which is centered over the western states can be seen entering the analysis

area on Fig. 1. A 60 m height fall over New Mexico is associated with its eastward movement. By 1200 GMT 19 March, the upper low deepened and moved eastward to northern Utah. This strengthens the southwesterly flow over Colorado and New Mexico (Fig. 2). Height falls of greater than 100 m in 12 hours are found over northern Colorado and southern Wyoming. By 0000 GMT 20 March, there are two upper lows. One is over western Nebraska (Fig. 3), while a residual low remains over Utah. This causes the flow to become much more westerly over the analysis area. Height falls of 120 m are found to the southeast of the low center over Nebraska, suggesting continued movement and development. In subsequent periods, the low continues moving northeastward across South Dakota and Minnesota and is located over northern Wisconsin by 1200 GMT 21 March.

B. SURFACE PATTERN

The composite surface pattern for the period is presented in Fig. 4. By 0000 GMT 19 March, surface frontogenesis occurs over the southern Rockies in association with the 500 mb low. The front then proceeds eastward into the Midwest and stretches from South Dakota to Texas on 20 March. The most active cyclone during the time period forms over New Mexico on the 19th and then moves across Kansas into Nebraska by the 20th. Although the 500 mb low was

intense, the surface cyclogenesis is modest, with only a 1000 mb central pressure.

C. JET STREAKS

Manual isentropic analyses will be utilized to describe the jet streak activity in this case. Fig. 5a displays a Montgomery stream function analysis along with the isotachs for 315K for 0000 GMT 19 March 1982. The Montgomery stream function is equivalent to height contours on a constant pressure chart. The pressure on the 315K surface is presented on Fig. 5b. Fig. 5c presents the Ri analysis for the 315-310K layer along with the mean height of the layer. The Ri was calculated using the height, wind, and temperature for each of the two levels listed following equation (1). Fig. 5d contains the components of the Ri, the wind shear and the thickness of the layer. The thickness of the layer is inversely related to the layer stability. The smaller the interval between two isentropic layers, the greater the layer stability. Thus, wind shear and stability for each layer can be evaluated from the analysis. The wind shear is in units of m/s per 300 m so that the operational meteorologist can approximate shear in knots/1000 ft by simply multiplying by two. Wind shear of 5 knots/1000 ft (2.5 m/s per 300 m) is an empirical threshold for light CAT (Lee et al., 1979).

The isentropic vertical structure for 0000 GMT 19 March (shown in Figs. 5-9) varies greatly from low to high levels. The geostrophic flow is southwesterly at all the isentropic levels 315 to 335K (Figs. 5a-9a). The flow is weak at the lower levels, but is more intense in the upper troposphere (see levels 325, 330 and 335K in Figs, 7a, 8a and 9a). The 335K analysis (Fig. 9a) shows the strong flow (75 m/s) in the lee of the Rockies as well as the intense flow (80 m/s) into and upstream of the ridge in Minnesota. The strong gradient over Minnesota is also influenced by the confluence of the flow to the north and south of the low. The main polar jet stream axis extends from northwest Colorado through Minnesota. The weaker lower lever jet streak axis over Missouri-Illinois (320-325K) is associated with the remnants of an old polar jet.

A steeply sloping, isentropic surface dominates the lower levels (315-320K). The 315K surface sloped upward from 720 mb over central Texas to 280 mb over Montana (Fig. 5b). The slope is the steepest over New Mexico, reflecting nearly adiabatic conditions as well as a strong horizontal temperature gradient. The south-to-north slope is less dramatic at 320K (Fig. 6b, 510-260 mb).

The upper levels (325-335K) has a more gentle south-to-north slope with only a 50 mb difference in pressure levels between central Texas to Montana at 335K (Fig. 9b) and 200

mb difference at 325K (Fig. 7b). The slope actually reverses over Iowa (Fig. 9b). The flat 335K pressure topography is typical near the tropopause. When using the pressure charts (Figs. 5b-19b), note that the contour intervals vary from 40 mb at 315K to 10 mb at 330K and 335K.

Three jet streaks are evident at 0000 GMT 19 March: the 75 m/s jet streak at 325K (Fig. 7a) over Colorado, the 80 m/s jet streak at 335K (Fig. 9a) which extends from South Dakota through Wisconsin and a 70 m/s jet streak at 335K (Fig. 9a) which extends from Missouri into Illinois. The main polar jet stream axis is at about 300 mb while the more southern jet is at about 210 mb.

At 1200 GMT 19 March, the polar jet stream axis has shifted further to the southeast over New Mexico, but slightly north and east over Minnesota. The weaker jet that was previously over Missouri moves east into Illinois outside of the analysis area.

In the lower isentropic levels, the strong south-to-north slope is still quite pronounced. At 315K (Fig. 10b), the isentropic surface slopes from 760 mb over Texas to 280 mb over Wyoming. The flow remains southwesterly all through the lower levels. The cyclonically curved Montgomery stream function contours over Colorado and Wyoming indicate the approaching upper low (Fig. 10a).

At the upper levels, the embedded jet streaks have a distinct signature on the 330K isotach analysis (Fig. 13a).

The jet streak over the Great Lakes moved east into southern Ontario and was responsible for many CAT reports. The jet streak over Colorado has moved southeastward while the jet streak over Missouri moved eastward. At 330K (Fig. 13b) a very tight isobaric gradient exists over Iowa. This is indicative of a very steep and intense upper front. Reports of CAT occurred in this area.

Major changes occur in the twelve-hour period to 0000 GMT 20 March. The slope of the isentropic surfaces decrease at both the upper and lower levels. The winds becomes more zonal at all levels (Figs. 15-19) as the upper ridge over the Midwest moved rapidly to the east. The major jet stream axis extends from northern New Mexico through northern Missouri. At the lower levels the upper front shows less slope. At 315K (Fig. 15b), the isentropic surface slopes from 680 mb over Oklahoma to 280 mb over Wyoming, compared to 740-280 mb during the previous time period.

At the upper levels, the slope of the upper front is also weaker. By 0000 GMT 20 March, the slope of the 330K surface over Iowa reduces from 60 mb to 40 mb. The jet streak, formerly over Ontario, moves eastward to just north of Michigan. The jet streak over southeastern Colorado moves east to the Oklahoma panhandle (Fig. 16b).

As the slope and strength of the upper front decreases and the flow becomes more zonal, the number of CAT reports also decrease. Since jet streaks moving into sharp troughs

and ridges is conducive to CAT, the evolution of flow into a more zonal orientation would be expected to decrease the likelihood of CAT. The wind shear associated with these jet streaks is instrumental in the development of the CAT. The wind shear and Richardson number associated with these jet streaks are discussed in the next chapter.

V. CAT ANALYSIS FROM MANUAL ANALYSES

The Richarson number (Ri), wind shear and stability analyses for this case study are discussed to determine the success of isentropic analysis for resolving atmospheric conditions responsible for CAT. CAT reports will be compared to Ri and shear analyses wherever possible. The mean height of each isentropic layer is included on panel c of Figs. 5-19 to determine in which layer the CAT report occurred. The mean height is determined by averaging the height of the two layers listed, e.g. Fig. 5c is the result of averaging the height of the 315K and 310K surfaces. The height of each level is determined by interpolating from radiosonde data. To interpret Figs. 5-19d, it is to be recalled that CAT quite often occurs in the sloping baroclinic zones and near the tropopause (stable areas) where the wind shear is a maximum. To reach the critical Ri of 0.25 requires the wind shear term to be large to overcome the effects of stability.

A. 0000 GMT 19 MARCH 1982

At 0000 GMT 19 March, two jet stream axes are evident. In general, the northern jet has its strongest Ri signature at lower levels (Figs. 5c-7c, 315-325K), while the weaker southern jet has its strongest signature at 335K (Fig. 9c). The areas of low Ri correspond very closely to the location

of the jet stream axes at lower levels and to the embedded jet streaks at higher levels (330-335K).

At 315K (Fig. 5c), there are two large areas of low Ri. One area of low Ri extends from the Rockies to the northern plains and is closely associated with the position of the northern jet. Two distinct minima of Ri are in New Mexico and Wyoming. Wind shear is quite large over New Mexico (as high as 9 m/s per 300 m), while a small isentropic layer thickness of only 400 m indicates stable air. The layer slopes steeply from 680 to 400 mb over New Mexico alone. There were five CAT reports at this level ranging from light to severe (Fig. 20, reports #2, #4, #12, #14 and #15). The severe report (#4) occurred over Colorado where the Ri was analyzed to be 2.8 and the wind shear is 2.5 m/s per 300m. One moderate (#2) and one light (#12) report occurred over New Mexico with Ri's of 2.5 and 2.0 and with wind shear values of 2.0 and 4.0 m/s per 300 m, respectively. One light (#14) and one light-to-moderate (#15) CAT report occurred over South Dakota and Montana, respectively. Both reports were in the area of low Ri's and strong wind shears.

The second area of low Ri at 315K over Kansas and Missouri is associated with the weaker southern jet stream axis that extends from Kansas through central Missouri. The wind shear over the area is 2-3 m/s per 300 m. There was one report of light-to-moderate CAT over Missouri (Fig. 20,

report #11). The Ri in the vicinity of the report is 0.8 while the wind shear is 3.0 m/s per 300m.

Moving upward to 320K (Fig. 6a), the jet axes are essentially in the same positions as at the 315K level. Low Ri values are found along the northern jet stream axis as well as with the weaker southern jet axis over Kansas and Missouri. The low Ri areas are about the same at both 315K and 320K. There were two CAT reports in this layer. One report over Utah (Fig. 20 report #1) was associated with the northern jet, while the other report was located in the area between the jet stream axes (Fig. 20, report #13). The moderate-to-severe report over Utah occurred in an area where the Ri was analyzed at 0.7 and the wind shear at 4.6 m/s per 300m. The Ri for the light-to-moderate report (#13) is 2.8 while the wind shear is 2.0. The area between the two jets is a favored area for the development of CAT (Lee et al. 1979).

AT 325K (Fig. 7a), both jet axes are easy to distinguish. The low Ri values were just to the south of both jets except for the area of low Ri over Montana which is north of the jet. The area of low Ri over Oklahoma is associated with the southern jet stream axis. There were no CAT reports in this layer.

At 330K (Fig. 8a), there is one large area of low Ri south of the main jet. Wind shears range from 2-4 m/s per 300 m over most of the area, but are as high as 7 m/s per

300 m over Wisconsin (off map). Three reports of light CAT (Fig. 20, reports #5, #7 and #9) and one report of moderate CAT (Fig. 20, report #3) were found at this level. There was also a report of no turbulence (Fig. 20, report #8) just to the north of the area of low Ri. The moderate CAT report (#3) over NW Iowa occurred in an area where the Ri is 0.8 and the wind shear is 3 m/s per 300 m. The light CAT report (#5) over South Dakota has an Ri of 1.0 and a wind shear of 3.7 m/s per 300 m. CAT report #9 (over Minnesota) has an Ri of 1.0 with a wind shear of 3.0 m/s per 300 m. The light CAT report over Montana (#7) occurred where the Ri was analyzed at 2.4 and the wind shear was 2.5 m/s per 300 m. Notice the very strong jet streak over Colorado (70 m/s), with the Ri remaining above 3.0. This can be explained by the smaller values of wind shear over the area (Fig. 8d). Wind shear tends to be the greatest in the sloping stable layer and also just above the tropopause.

At 335K (Fig. 9c) the area of low Ri over Missouri is associated with the southern jet axis, while the low Ri over Iowa and Minnesota is associated with the northern jet. Two reports of no turbulence occurred in this layer (Fig. 20, reports #6 and #10) over Oklahoma and Colorado, where the Ri is >3.0. There was also a report of light turbulence (Fig. 20, report #16) over Iowa in an area where the Ri is 2.0 and the wind shear is 2.0 m/s per 300 m.

B. 1200 GMT 19 MARCH 1982

At 1200 GMT, the polar jet stream is nearly stationary. The southern portion moved south and slightly east and the northern portion moved north and east. The southern jet axis jet is not as evident as the strongest portion has moved eastward out of the analysis area.

At 315K (Fig. 10c), the area of low Ri over New Mexico through Minnesota is once again located along the northern jet axis. There were five reports of CAT (Fig. 20 report #17 and #24-27). The two moderate-to-severe reports over Colorado (#17 & #24) both have wind shears of 4.0 m/s per 300 m while while the Ri ranges from 2.2-2.5. There were also two light-to-moderate (#25 & #26) and one light report (#27) that occurred the 315-310K layer. These CAT reports were all in areas of low Ri and strong vertical wind shear. The moderate-to-severe reports are from light aircraft and when normalized would be equivalent to a light-to-moderate report from a commercial airliner.

At 320K (Fig. 11c), there is only one significant area of low Ri associated with the jet streak over Minnesota. Low Ri would be expected here since a jet streak located in an upper ridge is a model relationship for the formation of CAT. There were no aircraft reports to confirm CAT in this layer.

The 325K Ri analysis (Fig. 12c) has three areas of low Ri. The area of low Ri in Minnesota is associated with the

jet streak located in the upper ridge. A small area of low Ri over Missouri as associated with the trailing edge of a jet streak, which had moved east out of the analysis area. The area of low Ri centered over the Oklahoma panhandle is southeast of the jet streak over the New Mexico-Colorado border. The area of low Ri over Minnesota is under a jet streak and is associated with strong wind shear (2-4 m/s per 300 m). One report of moderate CAT (Fig. 20, report #23) occurred over Minnesota.

The 330K Ri analysis (Fig. 13c) had only one area of low Ri. The area of low Ri over Minnesota and Iowa was related to the jet streak in the area with wind shears of >3 m/s per 300 m. However, there were no aircraft reports over the area, so the validity of this area can not be assessed.

At 335K (Fig. 14c), three areas of low Ri are analyzed. The small areas over north Texas and southwest Missouri are ahead of and south of the jet streak coming out of the southern Rockies. The area of low Ri over Minnesota and South Dakota is in the vicinity of the jet streak there. There were two reports of light-to-moderate CAT (Fig. 21, report #20 & #21) and two reports of light CAT (Fig. 21, report #18 & #19) over the Minnesota-Iowa border area. All reports occurred in areas where the Ri is less than 3.0 and the wind shear is 2.0 m/s per 300 m.

C. 0000 GMT 20 MARCH 1982

At 0000 GMT 20 March the polar jet became more zonal and extends from New Mexico through Iowa. A jet streak is centered over New Mexico at 315K (Fig. 16a) and over Kansas at 335K (Fig. 19a). The areas of low Ri are generally smaller in areal coverage and not as intense as during the two previous time periods. The CAT reports also taper off after 2200 GMT on the 19th.

At 315K (Fig. 15c), there are four small areas of Ri <3.0. The areas over New Mexico and Iowa are associated with the polar jet. One report of moderate CAT (Fig. 20, report #30) occurred at this level over northern New Mexico with the Ri of 2.5 and wind shear of 3.0 m/s per 300 m. The area of low Ri over Wyoming is associated with the strong shear that commonly occurs above the tropopause. This is a favored region for CAT occurrence (Lee et al. 1979). The area of low Ri over west Texas was just south of the jet.

The 320K Ri analysis (Fig. 16c) has only two small areas of low Ri. The one over Minnesota is north of the polar jet, while the one over Kansas is very near the jet stream core. At 325K (Fig. 17c), there is one small area of low Ri over Oklahoma. It is associated with the jet streak in the same area. There were no CAT reports at 320K or 325K.

The 330K Ri analysis (Fig. 18c) has three centers of Ri <3.0. The center over Minnesota is north of the polar jet and has strong wind shear (5 m/s per 300 m). The low Ri

over New Mexico and Missouri are near the polar jet axis. No confirming reports were available for these areas.

The 335K analysis (Fig. 19c) has one area of low Ri. The area extends both north and south of the jet axis. There was a report of light CAT (Fig. 20, report #29) over western Nebraska and a report of light-to-moderate CAT (#28) over Oklahoma.

The most encouraging result of this analysis is that all of the CAT reports were located in areas of low Ri and strong vertical wind shear. The results also show that both low-level and high-level CAT are depicted by the analysis. There are some areas of low Ri where no confirming reports of CAT were available. Although there were no confirming reports in these areas, they are synoptically consistent with the jet stream structure. The results also show that areas of Ri in the lower levels tend to follow the jet stream axis (Figs. 5 and 10) while the areas of Ri in the upper levels are more closely related to the embedded jet streaks (Figs. 8 and 13). One weakness in this study is that there were only 30 turbulence reports. Although this is a significant number of pilot reports to receive during a normal day, more reports would have been desirable to verify these analyses.

VI. ISENTROPIC CROSS-SECTION OBJECTIVE ANALYSIS MODEL

The purpose of objective analysis is to transfer meteorological observations to a regular grid as a means of eliminating subjectivity and enhancing timeliness of a analysis. Since Panofsky (1949) first proposed objective analysis to the meteorological community, many methods have been tried and tested. Due to the mesoscale nature of CAT, an objective analysis method that retains as much small scale detail as possible is essential. Petersen (1986) developed a three-dimensional objective analysis technique which is applicable to limited regions with abundant data. The Petersen objective analysis method capitalizes on the rich vertical resolution of the radiosonde by the use of isentropic cross-sections. Certain constraints were put on the analysis in order to produce a more accurate field. First, the analyses had to maintain hydrostatic balance. Also, vertical static stability must be positive and non-zero; otherwise, isentropes would cross one another. Additionally, the analyses had to maintain a smooth, continuous character over the entire field. This analysis model was used to see if it was a possible candidate to automate the analysis of CAT. This chapter will discuss the model formulation and output fields.

First, north-south cross-sections are produced over predetermined paths as illustrated in Fig. 21a. At each point where the vertical axes intersect a grid row, the locations of the grid row and values of pressure and moisture on each isentropic level are interpolated and stored. The Petersen method utilizes overlapping quadradic polynomials which connect successive data points exactly. When the entire area is analyzed in the north-south direction, a second set of cross-sections is then obtained along each grid row using the previously-derived intersection data. Grid values are thus obtained at each row-column intersection.

The next step is to compute hydrostatically the non-surface grid point values of the Montgomery stream function. The Montgomery stream function is found using:

$$\Psi_{m_{L+1}} = \Psi_{m_L} + Cp \times \Delta\theta \times (\bar{P}_\theta/1000)^k, \qquad (4)$$

where Cp is the specific heat of dry air at constant pressure, $\bar{P}_\theta$ is the mean pressure between isentropic levels L and L+1, $k = R_d/Cp$, and θ is the potential temperature difference between this isentropic surface and the one immediately below it (Petersen, 1986). Geostrophic wind estimates are then obtained using centered finite differences on the interior of the grid and two point forward/backward differences along the grid limits. Then the geostrophic components are interpolated bi-linearly back to the location of each observation. An estimate of the ageostrophic speed

departure and the normalized ageostrophic components are then calculated. They are then interpolated back to the grid using a cubic polynomial scheme. The ageostrophic wind is then added to the geostrophic speed computations to obtain the final wind analysis.

Two problems arise with this routine. One problem common to most objective analysis routines is the lateral boundary conditions. A linear extrapolation is made beyond the normal limits of the individual sections. This modification is necessary because the interpolating polynomial can be evaluated only at locations between observed data points (Petersen, 1986). The other problem is the intersection of the potential temperature surfaces with the ground. In regions where the surface potential temperature is greater than that of the isentropic surface being analyzed (i.e., the isentropic surface is underground), a vertical extrapolation is necessary (Petersen, 1986). The constraints that are imposed allow the isentropic surfaces to enter the ground and preserve surface frontal structure. This limits the influence of local low-level diurnal effects.

This objective analysis method was used to produce fields which were utilized to delineate areas of high CAT potential. The resulting analyses will be compared to the analyses that were hand drawn to see if they are consistent.

VII. COMPARISON OF MANUAL AND OBJECTIVE ANALYSES

In Chapter V, it was demonstrated that isentropic manual analyses provide excellent indications of where the greatest turbulence potential areas are located. In this chapter, the manual analyses will be compared to analyses produced by the Petersen objective analysis model. The objective and subjective analyses of the pressure of the pressure on the isentropic analyses compare very favorably. This is also true of the Montgomery stream function analyses. The objective pressure analysis was able to accurately capture the significant frontal features of this case. A good example of this is the steep frontal slope over Iowa at 330K (1200 GMT 19 March), discussed previously (compare Figs. 13 & 30). Since the subjective and objective pressure analyses and Montgomery stream function analyses agree favorably, they will not be discussed further in this chapter. Our attention will focus on the wind analyses and the derived CAT parameters of Ri and wind shear.

A. 0000 GMT 19 MARCH 1982

The objective analysis depicts the basic jet pattern well. The jet stream axis extending from New Mexico across Kansas and into Missouri, is indicated on both analyses (Figs. 5 & 22a). The jet streaks over Colorado and Minnesota

are also well depicted. The biggest difference in the analyses is the 60 m/s wind maximum over southwest New Mexico (Fig. 22a). The nearby radiosonde data and the manual analyses do not support the jet maxima. This poor analysis area is likely caused by a lateral boundary problem in the numerical analysis routine. Another weakness in the objective wind analysis is the isotach minimum of less than 20 m/s over Iowa (Fig. 22a). The hand analysis indicates the wind speed is 20-30 m/s (Fig. 5a). Note that this wind minimum is located entirely between radiosonde reporting stations. Since the Petersen analysis scheme analyzes exactly to the reporting station, any differences in analyses will be between the reporting stations. This difference arises because the objective wind analysis appears to force a spurious minimum in this area. The objective and hand analyses of Ri and wind shear for the 310-315K layer are in good agreement.

A comparison of the 320K analyses (Figs. 6 & 23) indicates good general agreement. The jet streaks over Colorado, Minnesota and Kansas are in the same position on both charts (Figs. 6a & 23a) and the wind speeds are essentially the same. The objective wind analysis again depicts a spurious maximum over southwestern New Mexico and an excessively broad minimum over Iowa. The Ri analyses (Figs. 6c & 23c) are in good general agreement with the exception of the area of low Ri over Kansas (Fig. 6c) and

the area of low Ri over Iowa (Fig. 23c). The objective Ri analysis did not extend a Ri minimum over western Kansas, however, light-to-moderate turbulence was reported over the area (Fig. 21, report #13). The strong Ri minimum area over Iowa (Ri 2.5) indicated by the objective analysis is suspect for a couple of reasons. First, it is located over a wind minimum, which synoptically, is not a likely location to find turbulence. Additionally, this small scale feature is located between the reporting stations at Peoria and Omaha in this area of poor objective wind analyses.

General agreement is once again evident at 325K (Figs. 7 & 24). The two problem areas from 315K and 320K still persist with the objective wind analyses being too weak over Iowa and in serious error over New Mexico. The problem over New Mexico is eapecially severe with wind ranging from 30 m/s over eastern New Mexico to greater than 80 m/s over western New Mexico. The objective analysis is not consistent with nearby radiosonde reports. El Paso reported 44 m/s and Albuquerque reported 52 m/s at this time period.

The 330K analyses (Figs. 8a & 25a) also indicates differences in the wind speed. Wind analyses over New Mexico and Iowa continues to be a problem. A new problem area appears over central and eastern Kansas as well as eastern Texas. The objective analysis indicates winds greater than 50 m/s over central Kansas while the radiosonde report over Kansas City was 40 m/s and the wind over Dodge City was 45

m/s. This 50 m/s wind maxima is not consistent with the jet stream structure. Also, the objective wind analysis of less than 30 m/s over eastern Kansas/western Missouri is not consistent with the surrounding data. Springfield Missouri, which is within 30 nm, reported a wind of 35 m/s. The eastern Texas objective minimum of less than 20 m/s was also inconsistent with nearby data. Longview, Texas reported winds of 24 m/s. These erroneous maxima and minima occur between stations and probably arise due to the polynomial interpolation in this complex case.

The Ri and wind shear analyses are generally in good agreement except for over southeastern Montana. The hand analysis (Figs. 9c & 9d) indicates the Ri is less than 3.0 and the wind shear greater than 2.0 m/s per 300 m whereas the objective analysis indicates Ri greater than 3.0 and the wind shear less than 2.0. Light CAT was reported over this area (Fig. 21, report #7). Three other CAT reports (#3, #5, & #7) occurred in areas where the Ri was analyzed low on both the manual and objective analyses.

The problem areas over New Mexico, Iowa, central Kansas, eastern Kansas and eastern Texas once again appear at 335K (compare Figs. 9a & 26a). Despite these problems, the objective wind analysis correctly depicts the jet streaks over Colorado and Minnesota as well as the jet streak over northern Missouri. The wind shear and Ri analyses (Figs 9c, d & 26 c, d) are in good agreement except for the Ri over

Minnesota. Low Ri is indicated by the manual analysis (Fig. 9c), but not on the objective analysis (Fig. 29c). There were no CAT reports over Minnesota to indicate which analysis is more reasonable.

B. 1200 GMT 19 MARCH 1982

At 315K, both analyses (Figs 10a & 27a) show the jet stream axis extending from New Mexico through the Dakotas and then sharply turning over the ridge. The largest difference in the analyses is over Missouri. The objective wind analysis of greater than 50 m/s over Missouri is impossible to support with the conventional data. Nearby radiosonde stations indicate winds considerably weaker over this area. This small scale area is once again located between reporting stations. The Petersen scheme is showing a tendency to overshoot relative minimum and maximum areas. Note on Fig. 10, there was a relative minimum over Arkansas, a relative maximum over Missouri, a relative minimum over Iowa and then another relative maximum over southern Canada. The Petersen routine seems to overestimate these relative minimums and maximums creating erroneous small scale features such as the maximum over Missouri. A local maximum does indeed exist over Missouri, but it is not as strong as indicated by the objective analysis. The Ri and wind shear analyses are in good agreement indicating low Ri and a strong shear zone with the primary jet axis.

General agreement is once again evident at 320K (Figs. 11 & 28). The problem area over Missouri is still present. Additionally, the objective analysis over Nebraska and New Mexico depicts two seperate jet maxima. This does not agree with the manual analysis. Considering continuity from the previous time period (0000 GMT 19 March), it is not likely that there are two separate jet streaks as depictied on the objective analysis. The North Platte radiosonde report was missing, which may account for why the analysis was suspect in this area. The Ri and wind shear analyses compared well however.

At 325K, there is good general agreement between all the analyses (Figs. 12 & 29). The objective wind analysis over western Nebraska again differs from the manual analysis. Additionally, the objective routine analyzed a small scale feature over Arkansas-Missouri. Synoptically, there appears to by no justification for this feature. The objective analysis also indicates a wind of less than 10 m/s over Montana at both 325K and 320K. The objective analysis correctly identifies that this was a relative minimum, but it overestimates the value of the minimum. The moderate turbulence report over Minnesota (Fig. 20, report #23) occurred where both analyses had areas of low Ri.

At 330K, two new differences are apparent (compare Figs. 13a & 30a). The objective scheme analyzes jet streaks of >50 m/s over Oklahoma and Missouri. The reported wind at

Amarillo was 47 m/s and at Oklahoma City it was 45 m/s, making the 50+ m/s analysis over Oklahoma hard to justify. The objective analysis of winds greater than 50 m/s area over Missouri is even less likely. The reported wind over Kansas City at this time was 41 m/s while the reported wind over Springfield was 32 m/s. The questionable area over Montana is evident at 330K also. The Ri analyses (Figs. 13c & 30c) vary greatly. The objectively analyzed jet streak over Oklahoma induces an area of low Ri which is not reflected in the manual analysis. The objective analysis of wind shear places a wind shear of greater than 10 m/s per 300 m over South Dakota. This area is very suspect, since the Huron radiosonde was missing for this time period. There were no CAT reports at this level to substantiate the areas of low Ri.

At 335K, there is once again large differences between the hand analysis (Fig. 14) and the objective analysis (Fig. 31). The 60+ m/s objective wind analyzed over Missouri is especially noticable. The observation at Kansas City was 47 m/s while the report over southwestern Missouri was 42 m/s. The objective analysis correctly places the position of the relative maximum, but once again overestimated its value. The Ri analyses were vastly different (compare Figs. 14c & 31c). The Ri objective analysis over Colorado is greatly influenced by the large area of wind shear (Fig. 31d) produced by the Petersen routine. This area is extremely

doubtful considering the Denver radiosonde was missing. Missing stations seem to allow the objective analysis routine too much freedom in estimating the wind field.

C. 0000 GMT 20 MARCH 1982

The 315K manual analysis (Fig. 15) indicates the jet streak is centered over New Mexico with the jet axis extending across the Oklahoma panhandle. This position was consistent with the previous position further west. However, the objective analysis (Fig. 32a) indicated a wind minimum of less than 30 m/s over the Texas panhandle with the main jet streak split into new centers, over Colorado and New Mexico. Other than the spurious minimum over Oklahoma, the wind analysis showed the general pattern correctly. Once again, the Denver sounding was missing and most likely led to the poor Colorado wind analysis. The manual Ri areas are in general agreement with the objective analysis (compare Figs. 15c & 32c). As expected, the wind shear analyses varied greatly since the isotach analyses differed so much.

At 320K, the objective analysis maintains the spurious wind minimum over the Oklahoma panhandle at 320K (compare Figs. 16a & 33a). Otherwise, the wind analyses are in general agreement. Both of the Ri analyses showed areas of low Ri over Kansas and Minnesota (Figs. 16c & 33c).

The poor objective wind analysis over the Oklahoma panhandle once again appears at 325K (compare Figs. 17a & 34a). Both analyses show areas of low Ri over Oklahoma (Figs. 17c & 34c). However, the manual analysis indicates a continuous area of low Ri from Oklahoma to Louisiana, whereas the objective analysis has two distinct areas. No CAT was reported in this area. This could have been the result of a lateral boundary problem.

At 330K, the objective analysis once again places a wind minimum in the same general area as below (Fig. 34a). The center of the jet streak on the objective analysis is over Oklahoma, while the center of the jet streak on the manual analysis (Fig. 18) is over Kansas. The reported winds of 61 m/s over Dodge City and a 53 m/s report over Oklahoma City, make it hard to justify the objective analysis position. The Ri analyses agree except over New Mexico where the hand analysis captures a small area of low Ri that is missed by the objective analysis.

At 335K, the wind speed problems over Texas and Colorado continue (compare Figs. 19a & 36a). The objective wind shear analysis once again showed a strong value over the missing Denver radiosonde. This strong wind shear analysis caused a large difference in the Ri analysis as well. The objective analyses had an area of low Ri over Colorado, whereas the manual analysis did not.

From studying the entire three time periods, it becomes apparent the largest problems with the objective analyses occur with the wind speed. In many areas the trend was correct, but the scheme tends to overestimate the absolute value of the relative minimum or maximum. This is especially true in areas where radiosonde data are missing or in areas located between reporting stations. In addition, lateral boundary problems are found over New Mexico and Louisiana.

VIII. SUMMARY AND CONCLUSIONS

Manual isentropic analyses were completed for a 24-h CAT outbreak over the midwestern region of the United States, for the purpose of delineating areas of high CAT potential. The analyses were then compared to CAT reports. Objective isentropic analyses, using a scheme developed by Petersen (1986), were then completed for the same time period and for the same fields. The objective analysis was derived from cross-sections which run north-south through the analysis area. Using cross-sections, the data were then interpolated to a regular grid using overlapping polynomials.

Objective and manual analyses produced derived parameters to delineate areas of high CAT potential and the associated jet stream structure. The parameters are the gradient Richardson number (Ri), the vertical wind shear, the mean height of the isentropic layer and the isentropic layer thickness. The analyses were computed at 5K intervals for layers covering most of the troposphere. CAT reports used for verification were obtained from the Air Force Global Weather Central (AFGWC) for the 24-h period of the CAT outbreak.

The manually analyzed Ri fields and high wind shear areas, computed from radiosonde data, were verified using the AFGWC CAT reports. The results of this verification are

encouraging. All the reports of CAT occurred in areas of low Ri and significant wind shear. However, the number of low Ri areas exceeded the coverage of the verifying reports. Most of the CAT likely areas that could not be verified are consistent with the isentropic jet stream and jet stream structure.

The Petersen objective analyses were compared to manual analyses to determine the skill of the objective analyses in delineating areas of high CAT potential. The analyses and Montgomery stream function analyses compared very well. The Ri, the wind shear and the wind speed analyses depict the general patterns well. The objective analysis tend to induce small scale spurious areas of CAT in several different ways. One problem is overestimating the value of the relative minima and maxima. The position of the minima and maxima are good, but the absolute value tends to be too low or high, repectively. Another source of error occurred in areas where the radiosonde data are missing. The quadratic polynomials used by the Petersen routine did not perform well in these data sparse regions. Finally, poor wind analyses did occur along the lateral boundaries.

Since this pilot study shows a good relationship between the hand analyzed Ri field and reports of CAT, further research should be undertaken to modify the Petersen wind interpolation and to continue to verify the isentropic approach for many different cases. Other objective methods

could be tested to see if they are more suitable to CAT analyses. AFGWC just started receiving pilot reports from the Regional Air Traffic Control Centers. This will mean a vast improvement in the quantity of pilot reports available to verify areas of high CAT potential. These reports, which are plotted at AFGWC could be archived so that many more cases of CAT outbreaks could be identified and analyzed. This is necessary to compile meaningful data relating the occurrences of CAT with analyzed Ri fields. The continued application of modern objective analysis techniques to the jet stream structure and CAT problems is required before reliable objective CAT analyses and forecasts are developed.

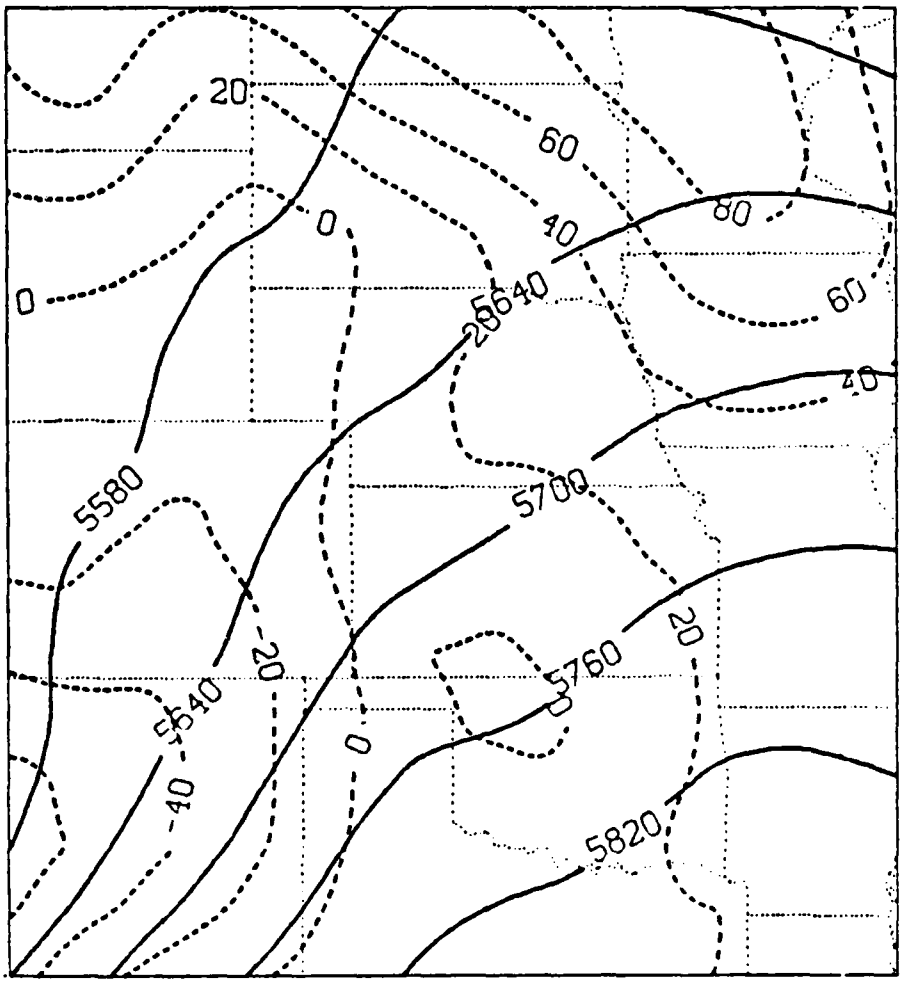

Fig. 1. 500 mb Heights (solid) and 1000-500 mb Thickness (dashed) for 0000 GMT 19 March 1982.

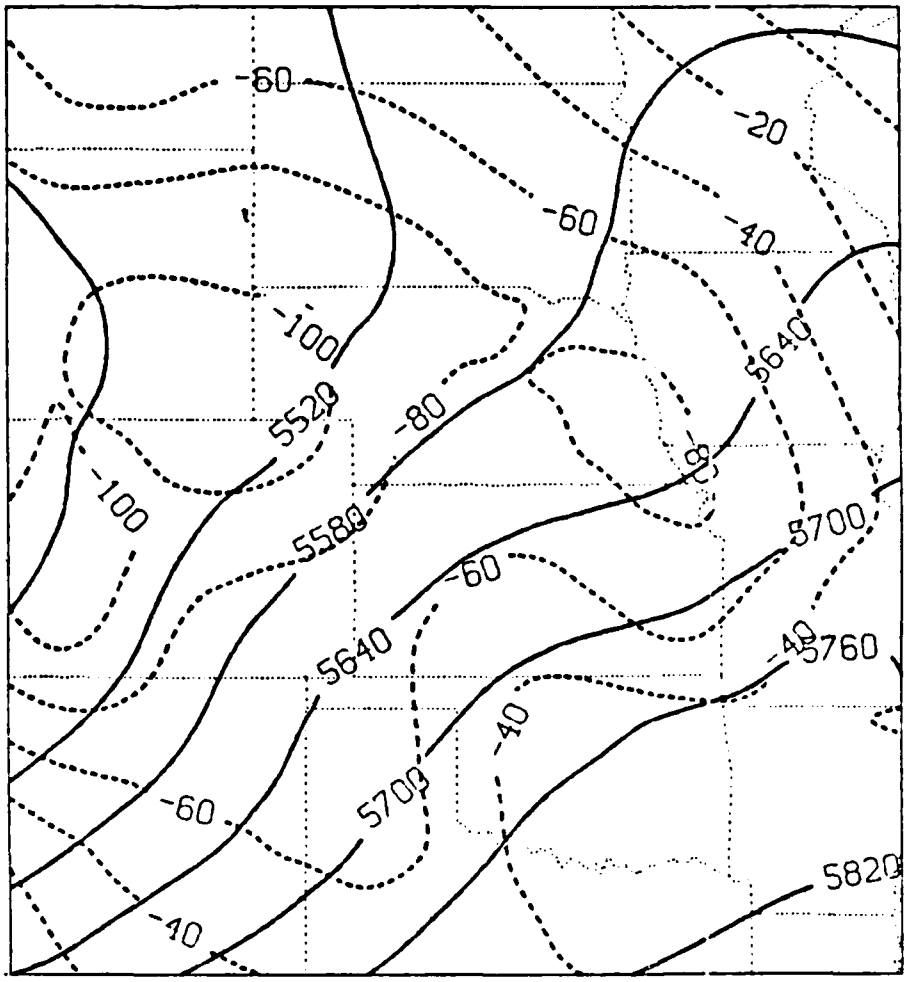

Fig. 2. 500 mb Heights (solid) and 1000-500 mb Thickness (dashed) for 1200 GMT 19 March 1982.

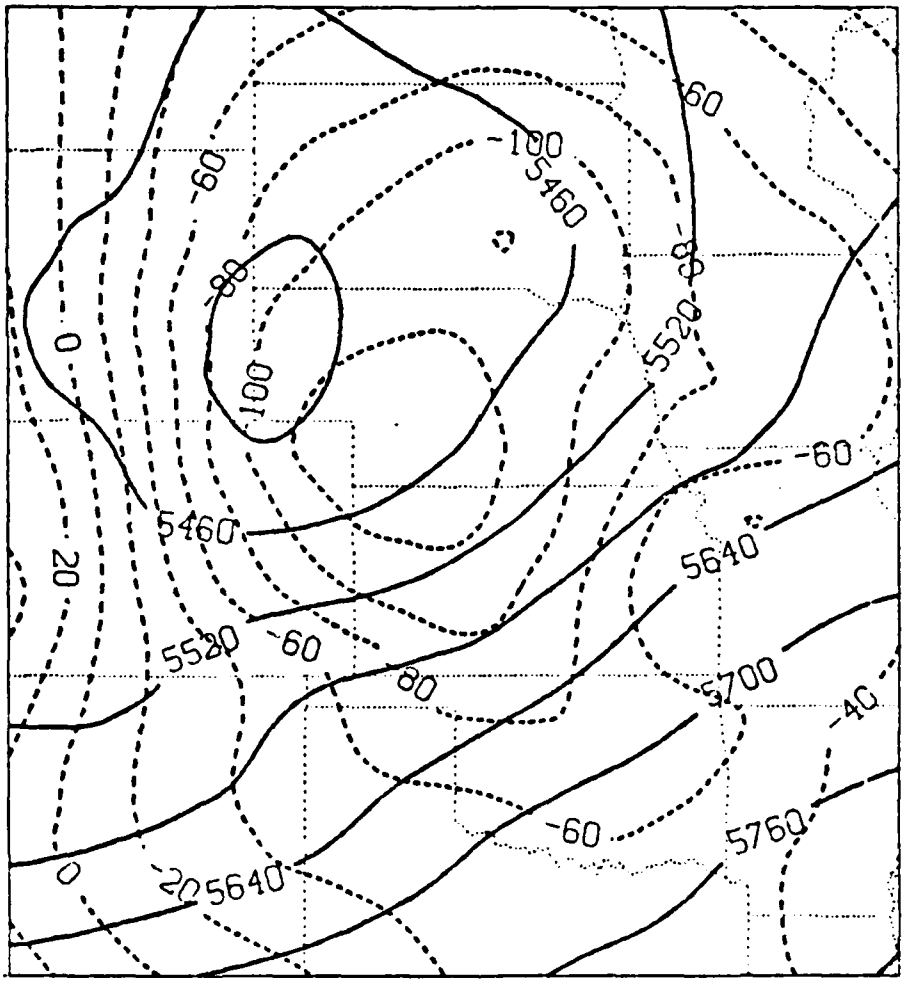

Fig. 3. 500 mb Heights (solid) and 1000-500 mb Thickness (dashed) for 0000 GMT 20 March 1982.

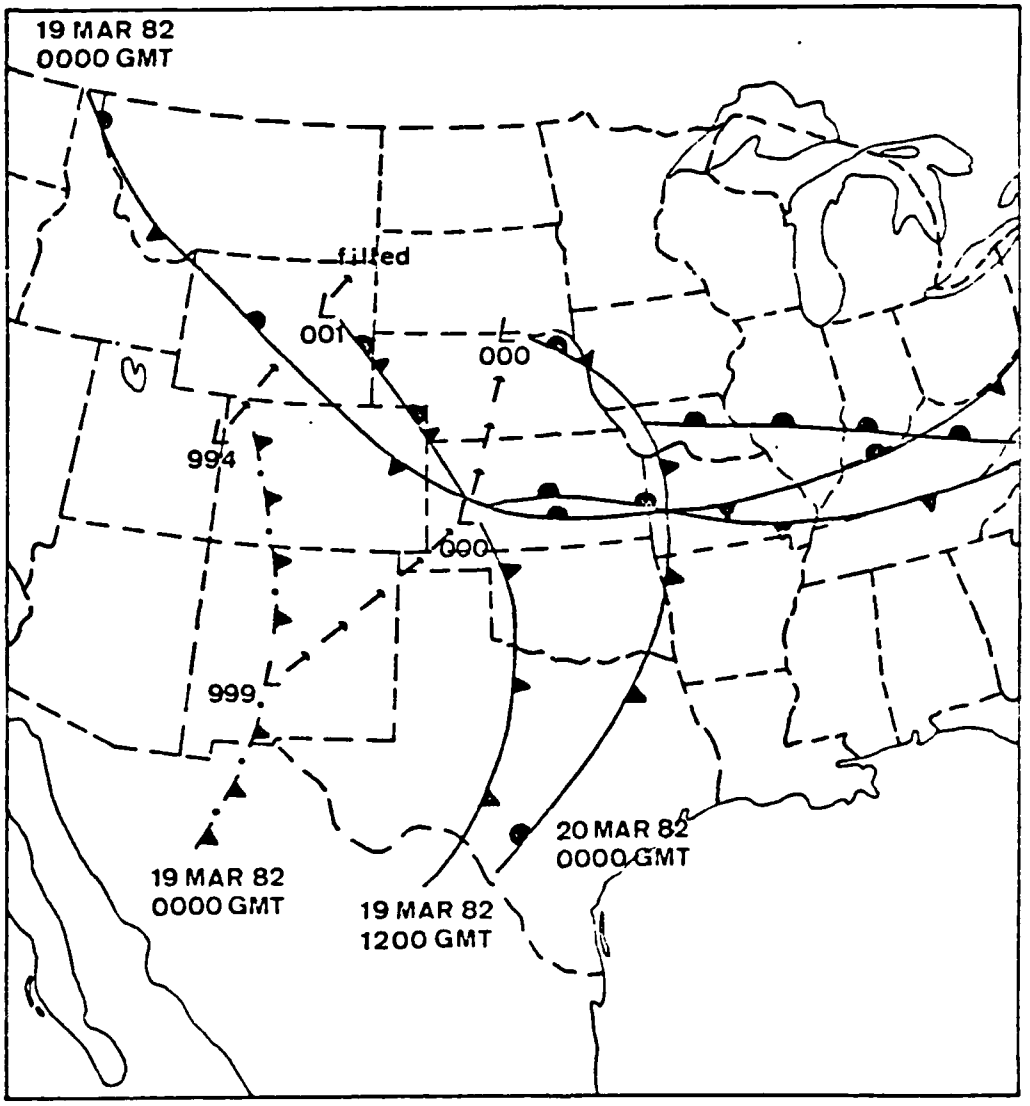

Fig. 4. Composite Surface Analysis for 0000 GMT 19 March 1982 through 0000 GMT 20 March 1982.

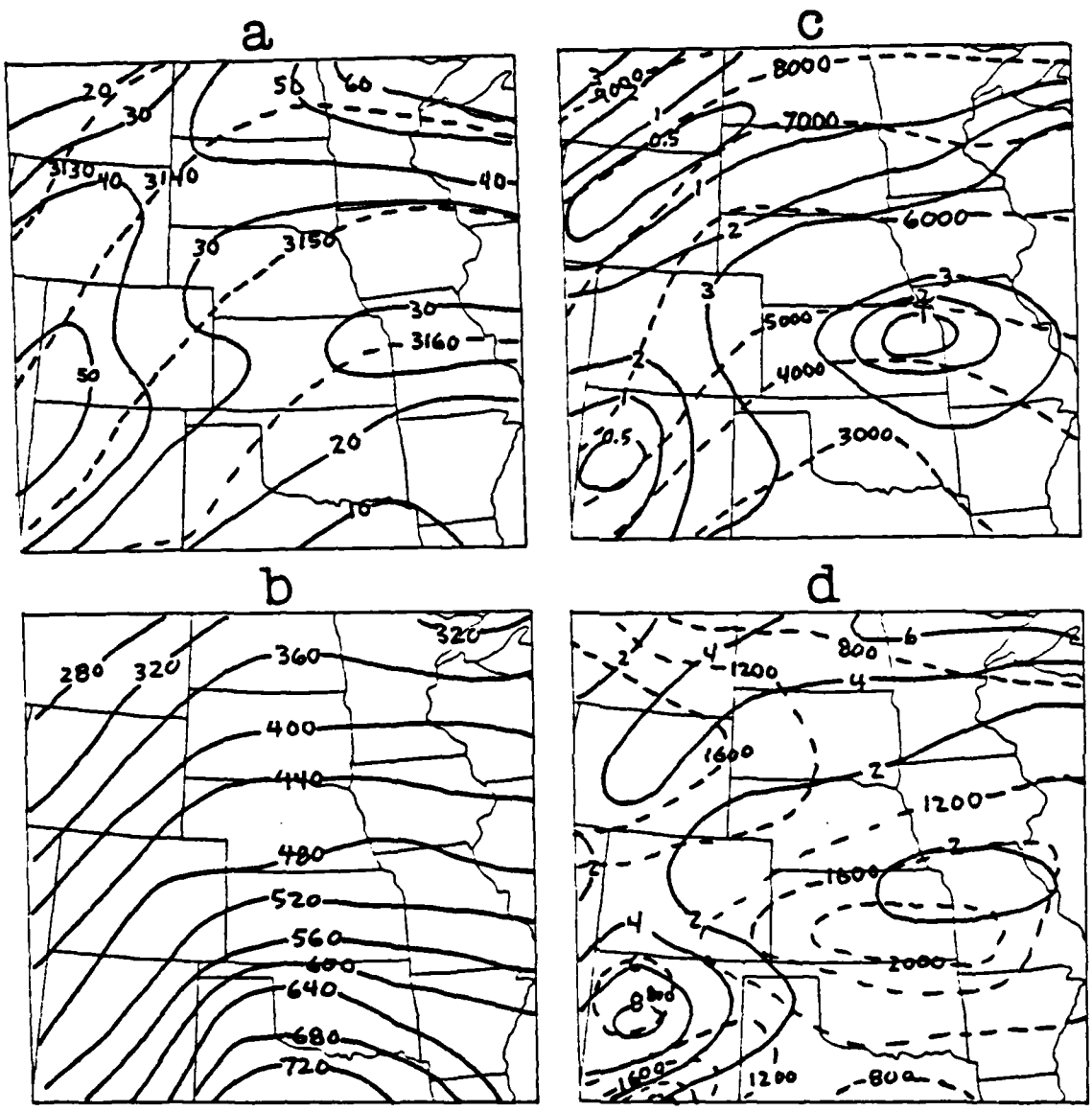

Fig. 5. Manual Analyses for 315K and 315-310K Richardson Number (Ri) 0000 GMT 19 March 1982 (a) Isotachs in m/s (solid) and Montgomery Stream Function in m^2/s^2 (dashed) (b) Pressure in mb. (c) Layer Ri (solid) and Mean Layer Height in m (dashed). (d) Layer Wind Shear in m/s (solid) and Layer Thickness in m (dashed).

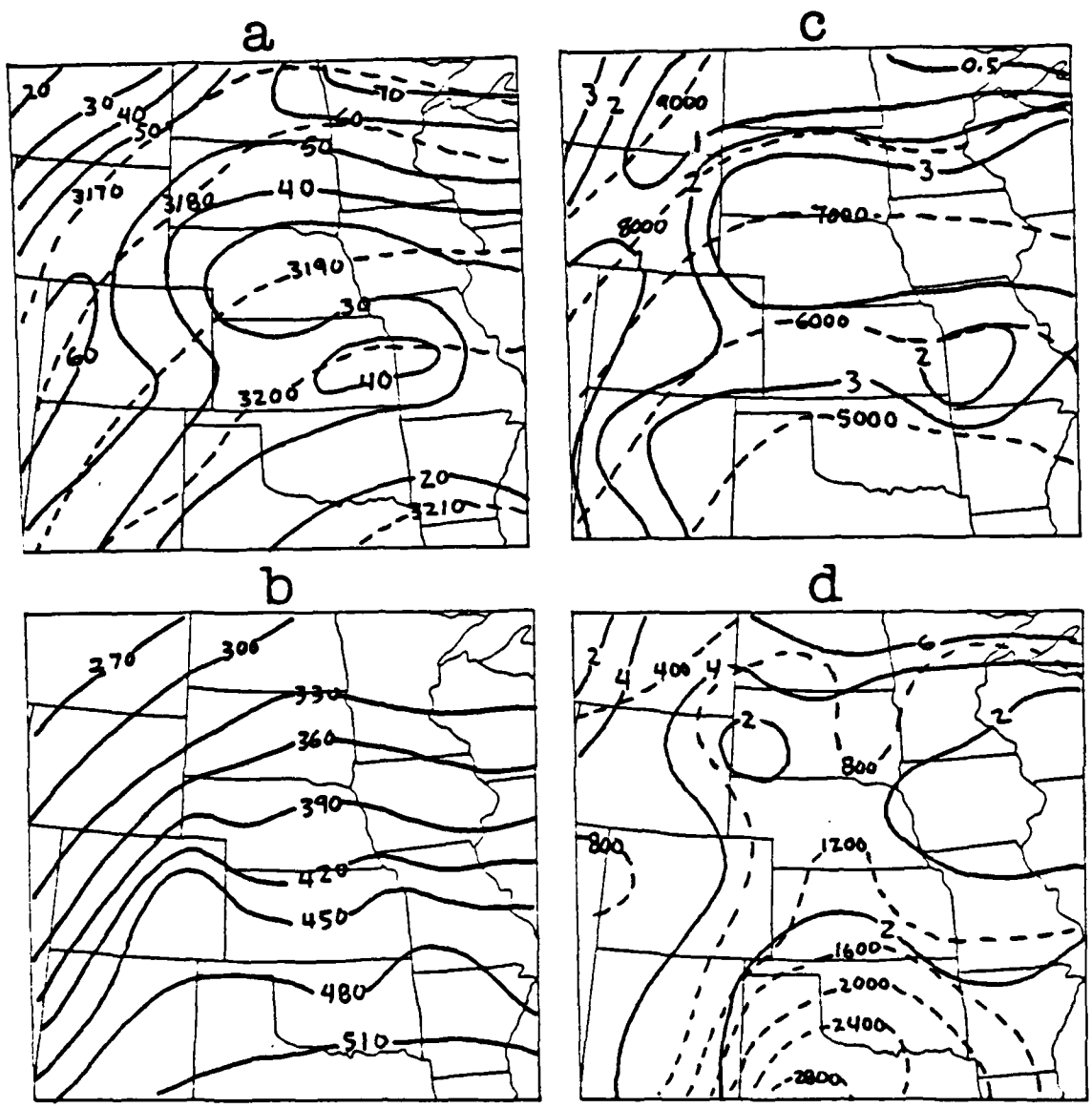

Fig. 6. Manual Analyses for 320K and 320-315K Richardson Number (Ri) 0000 GMT 19 March 1982 (a) Isotachs in m/s (solid) and Montgomery Stream Function in m^2/s^2 (dashed) (b) Pressure in mb. (c) Layer Ri (solid) and Mean Layer Height in m (dashed). (d) Layer Wind Shear in m/s (solid) and Layer Thickness in m (dashed).

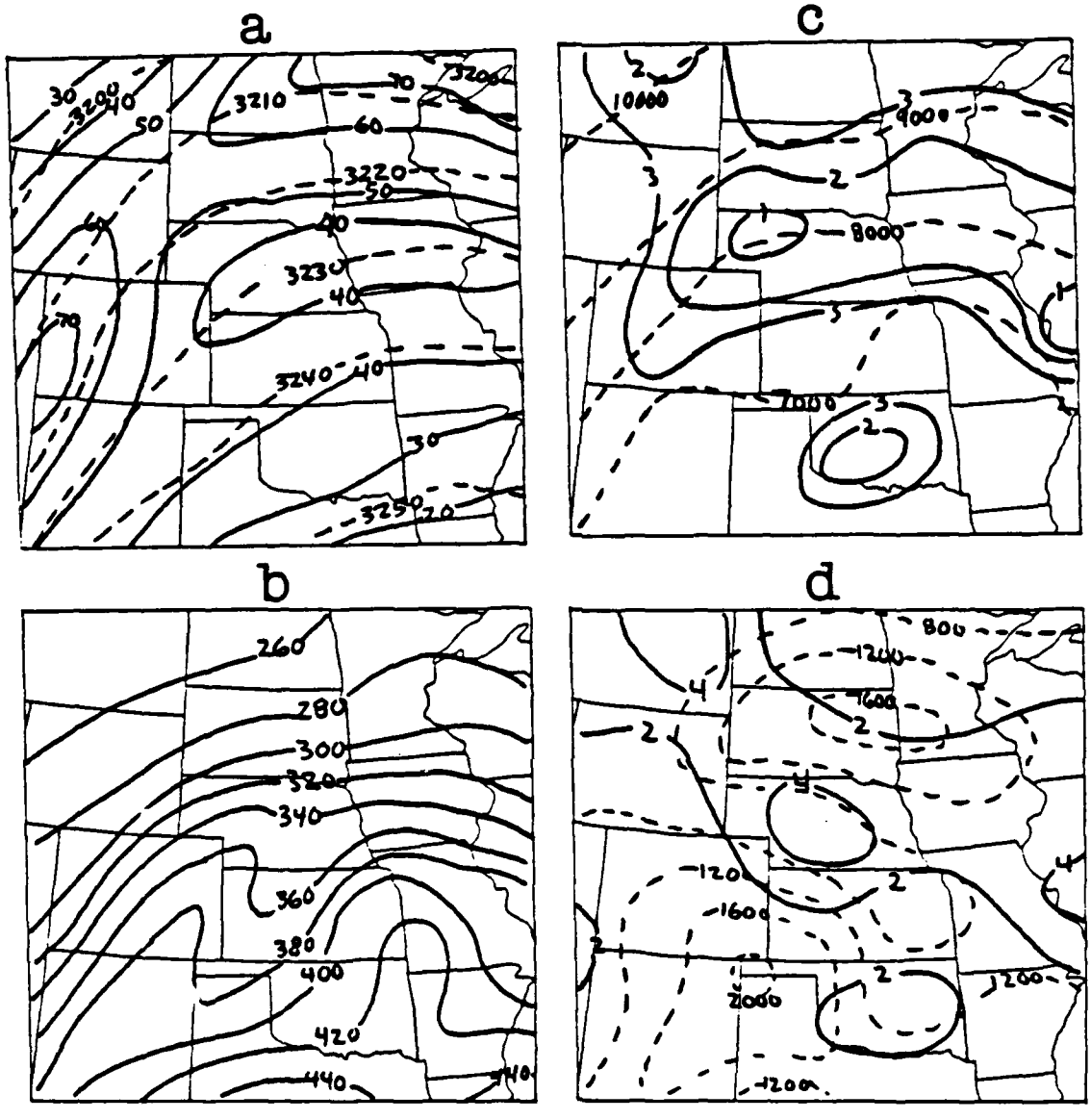

Fig. 7. Manual Analyses for 325K and 325-320K Richardson Number (Ri) 0000 GMT 19 March 1982 (a) Isotachs in m/s (solid) and Montgomery Stream Function in m^2/s^2 (dashed) (b) Pressure in mb. (c) Layer Ri (solid) and Mean Layer Height in m (dashed). (d) Layer Wind Shear in m/s (solid) and Layer Thickness in m (dashed).

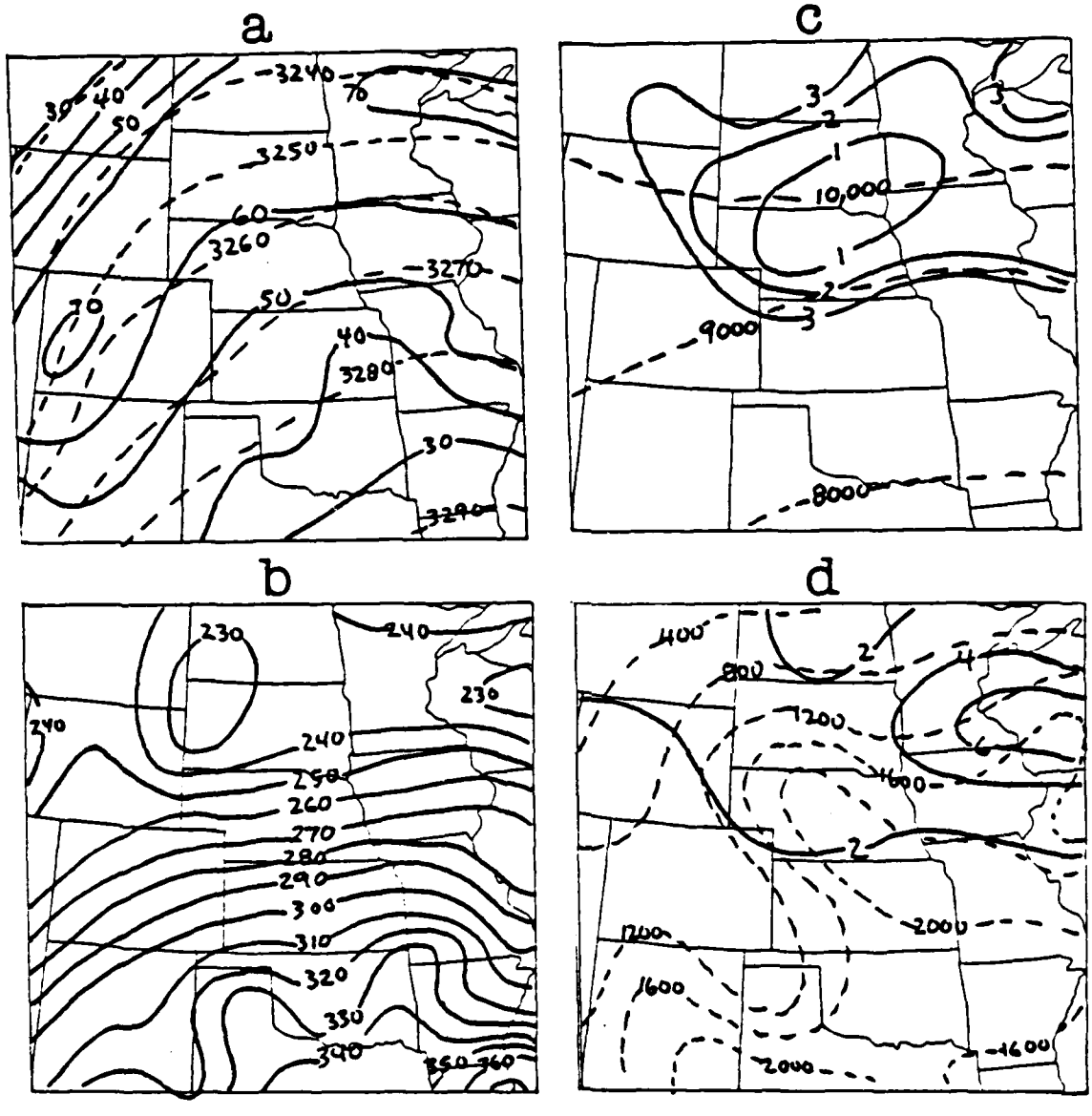

Fig. 8. Manual Analyses for 330K and 330-325K Richardson Number (Ri) 0000 GMT 19 March 1982 (a) Isotachs in m/s (solid) and Montgomery Stream Function in m^2/s^2 (dashed) (b) Pressure in mb. (c) Layer Ri (solid) and Mean Layer Height in m (dashed). (d) Layer Wind Shear in m/s (solid) and Layer Thickness in m (dashed).

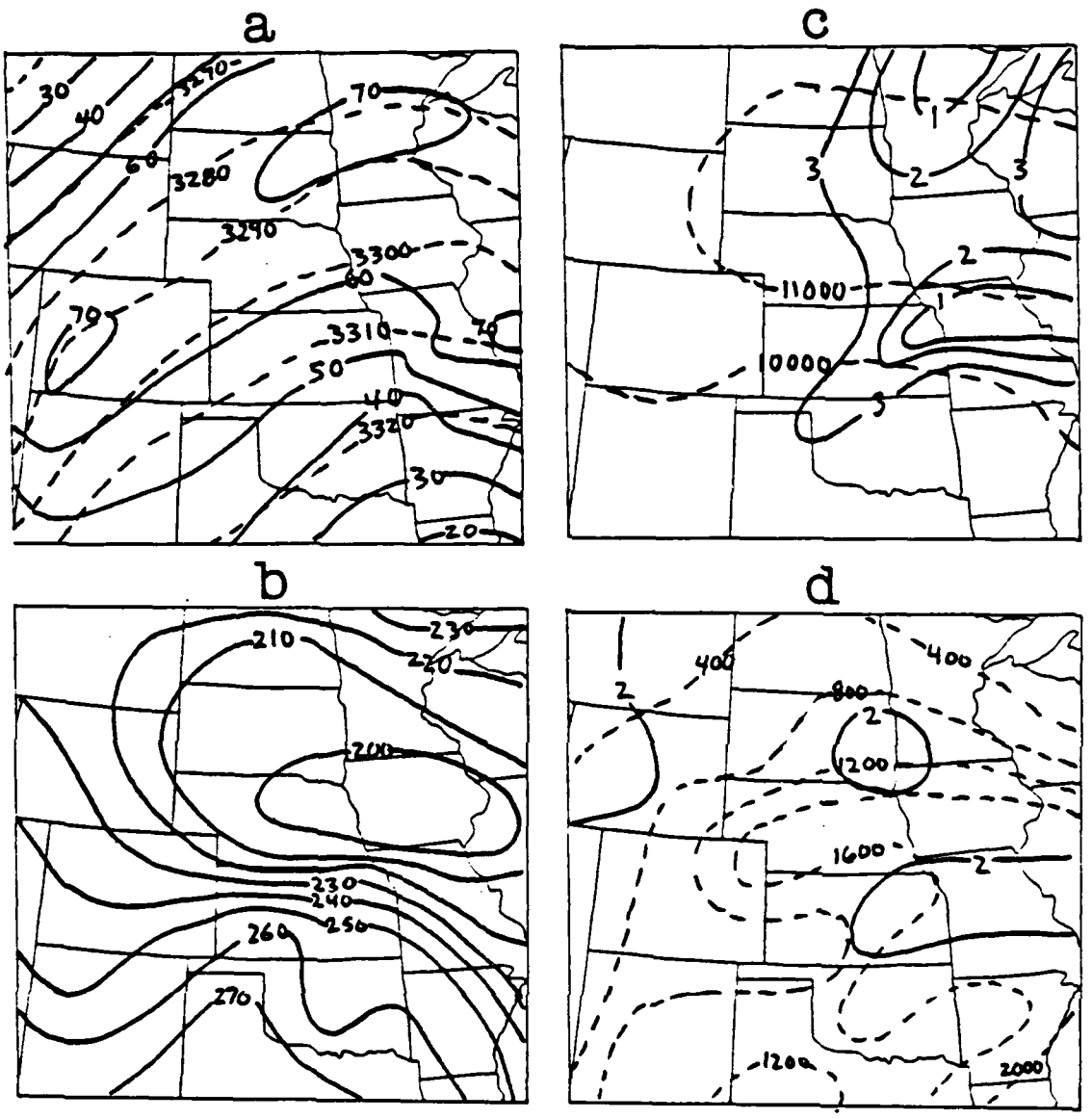

Fig. 9. Manual Analyses for 335K and 335-330K Richardson Number (Ri) 0000 GMT 19 March 1982 (a) Isotachs in m/s (solid) and Montgomery Stream Function in m^2/s^2 (dashed) (b) Pressure in mb. (c) Layer Ri (solid) and Mean Layer Height in m (dashed). (d) Layer Wind Shear in m/s (solid) and Layer Thickness in m (dashed).

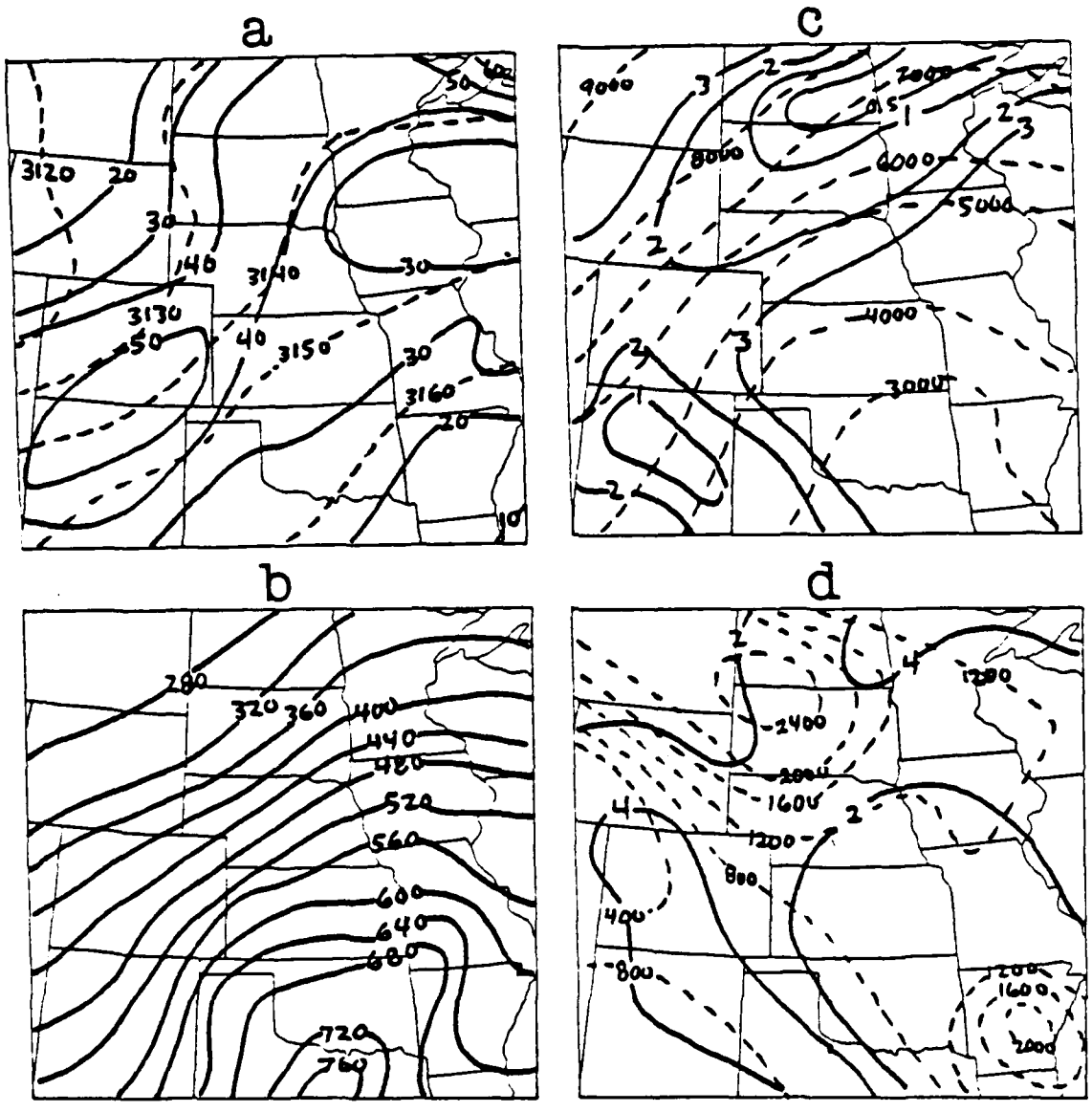

Fig. 10. Manual Analyses for 315K and 315-310K Richardson Number (Ri) 1200 GMT 19 March 1982 (a) Isotachs in m/s (solid) and Montgomery Stream Function in m^2/s^2 (dashed) (b) Pressure in mb. (c) Layer Ri (solid) and Mean Layer Height in m (dashed). (d) Layer Wind Shear in m/s (solid) and Layer Thickness in m (dashed).

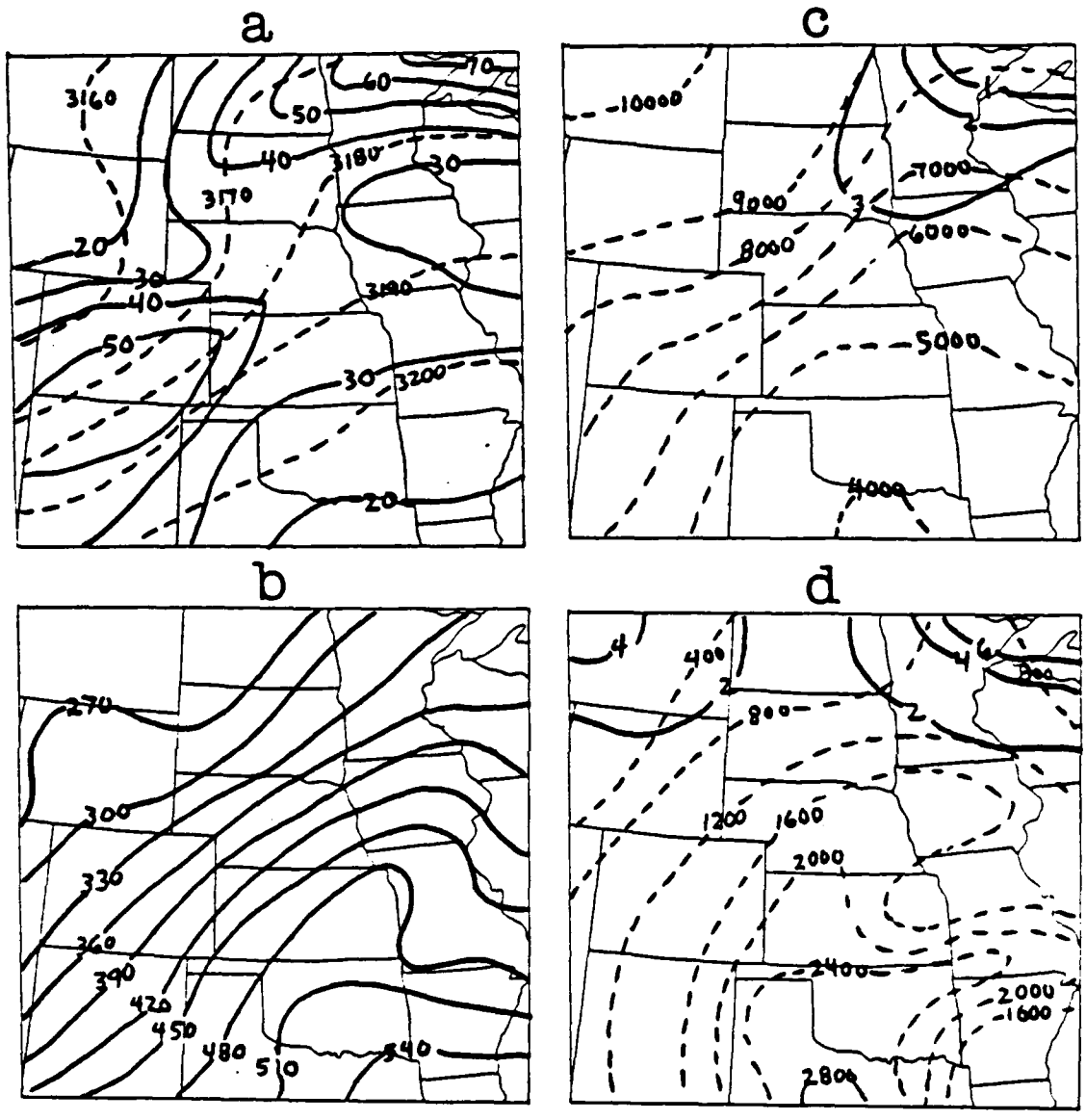

Fig. 11. Manual Analyses for 320K and 320-315K Richardson Number (Ri) 1200 GMT 19 March 1982 (a) Isotachs in m/s (solid) and Montgomery Stream Function in m^2/s^2 (dashed) (b) Pressure in mb. (c) Layer Ri (solid) and Mean Layer Height in m (dashed). (d) Layer Wind Shear in m/s (solid) and Layer Thickness in m (dashed).

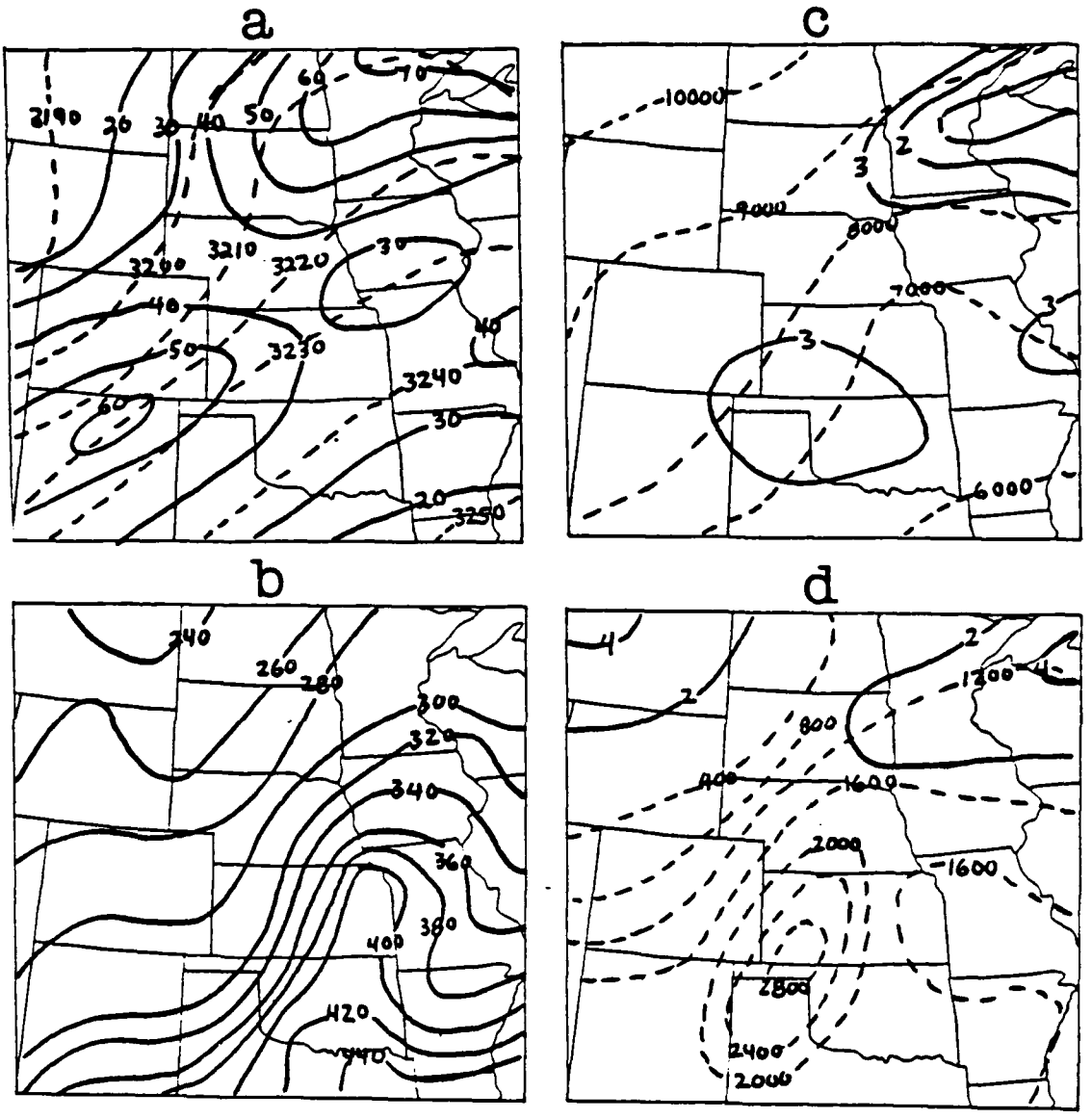

Fig. 12. Manual Analyses for 325K and 325-320K Richardson Number (Ri) 1200 GMT 19 March 1982 (a) Isotachs in m/s (solid) and Montgomery Stream Function in m^2/s^2 (dashed) (b) Pressure in mb. (c) Layer Ri (solid) and Mean Layer Height in m (dashed). (d) Layer Wind Shear in m/s (solid) and Layer Thickness in m (dashed).

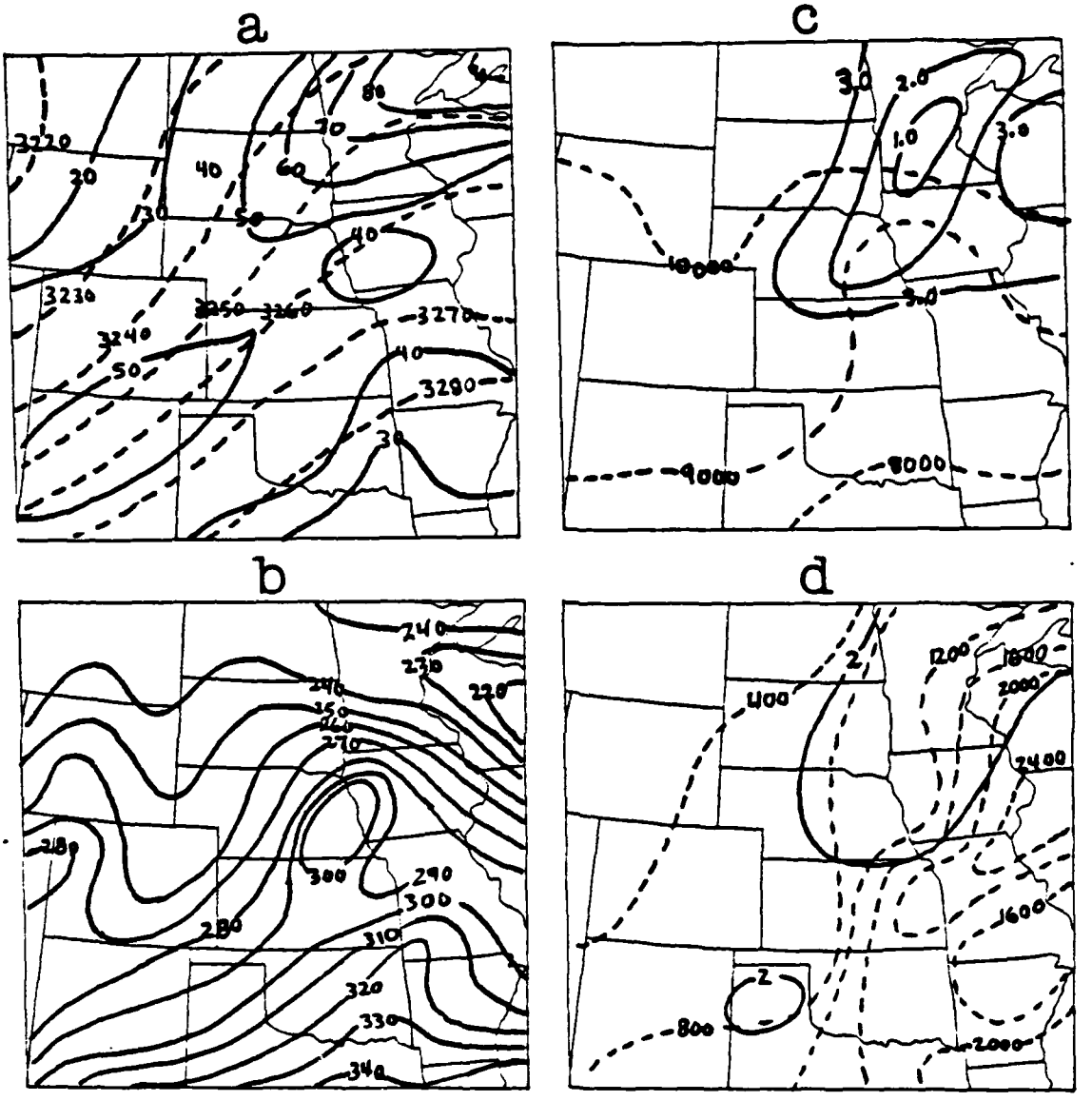

Fig. 13. Manual Analyses for 330K and 330-325K Richardson Number (Ri) 1200 GMT 19 March 1982 (a) Isotachs in m/s (solid) and Montgomery Stream Function in m^2/s^2 (dashed) (b) Pressure in mb. (c) Layer Ri (solid) and Mean Layer Height in m (dashed). (d) Layer Wind Shear in m/s (solid) and Layer Thickness in m (dashed).

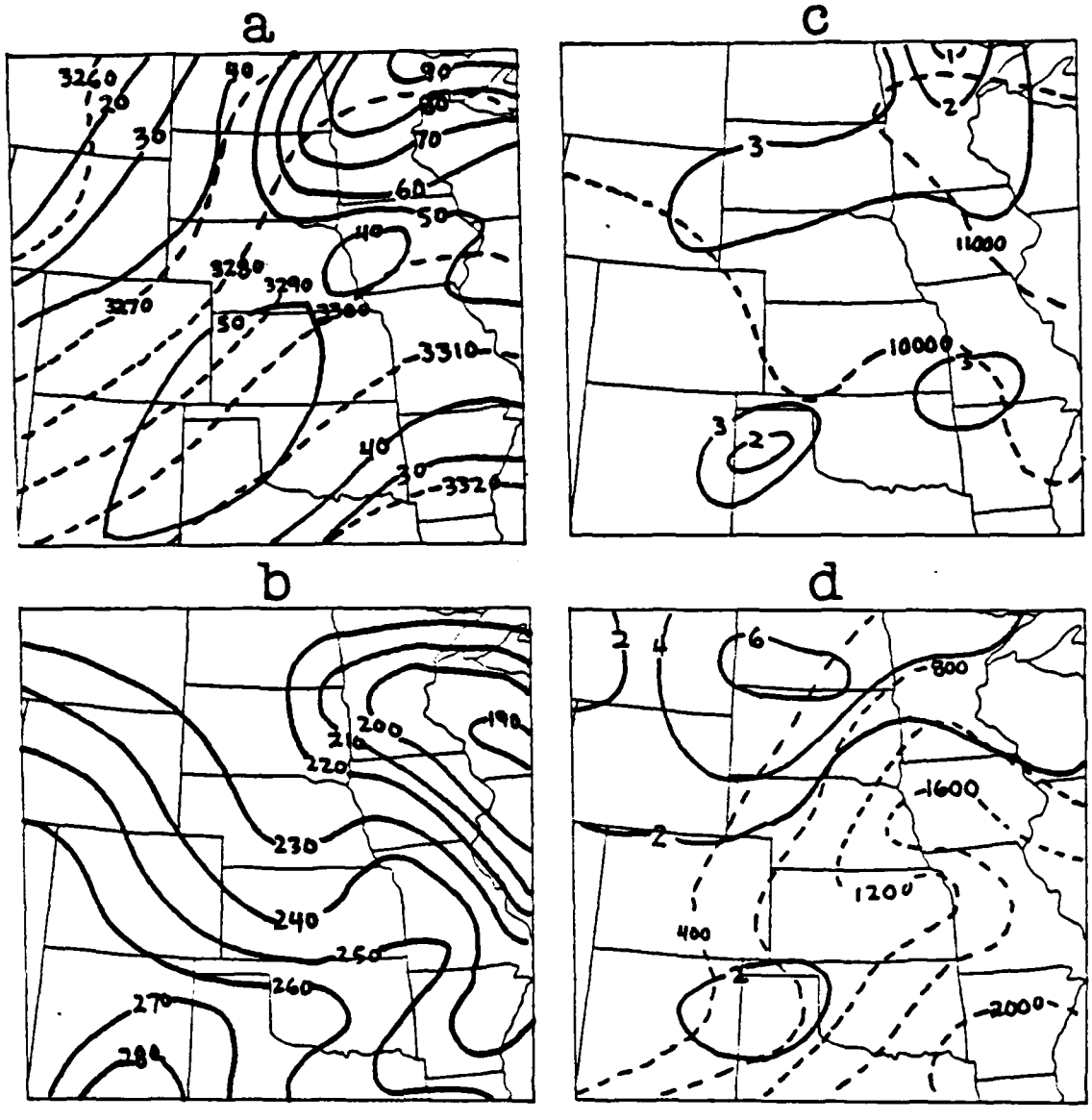

Fig. 14. Manual Analyses for 335K and 335-330K Richardson Number (Ri) 1200 GMT 19 March 1982 (a) Isotachs in m/s (solid) and Montgomery Stream Function in m^2/s^2 (dashed) (b) Pressure in mb. (c) Layer Ri (solid) and Mean Layer Height in m (dashed). (d) Layer Wind Shear in m/s (solid) and Layer Thickness in m (dashed).

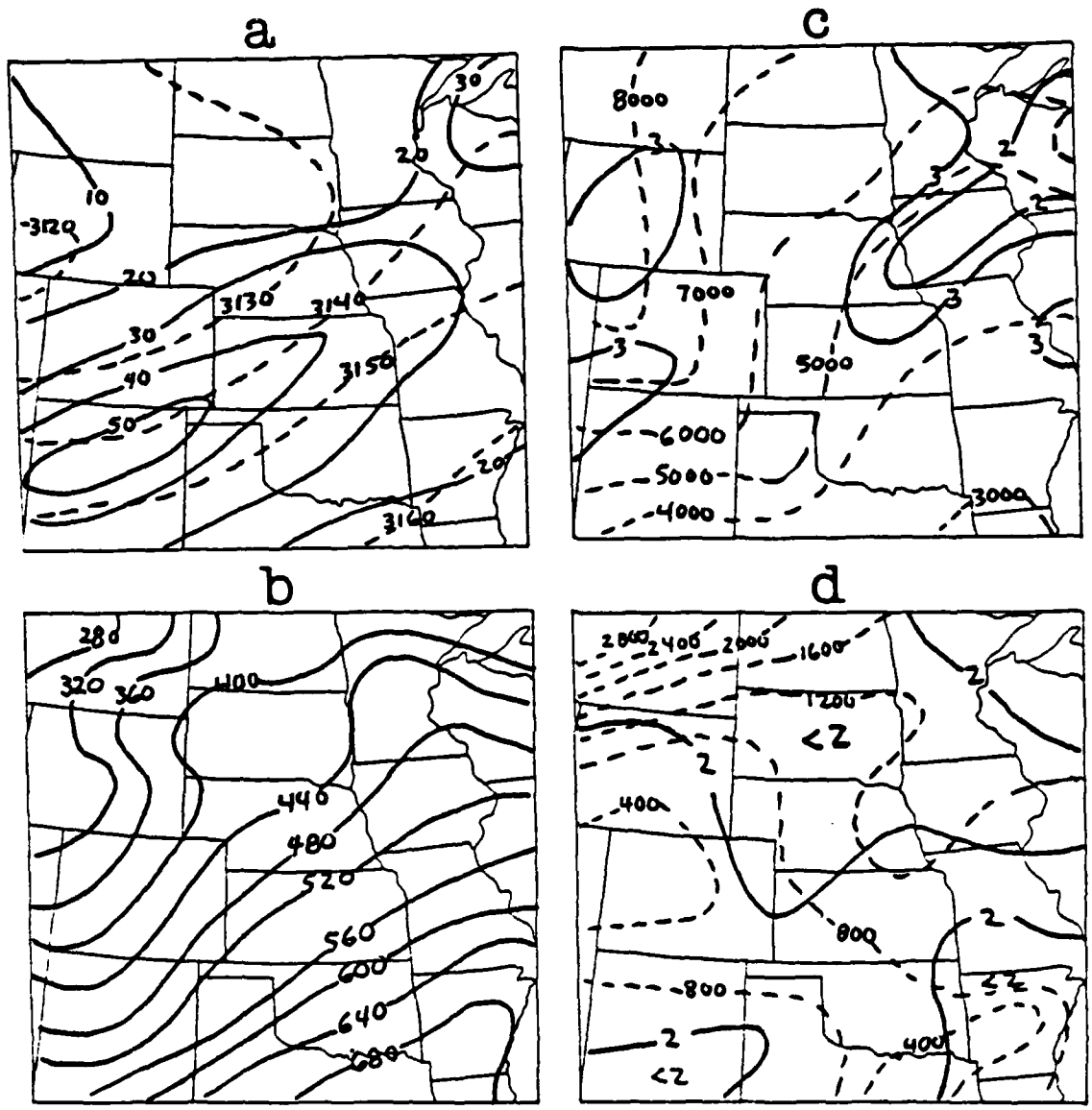

Fig. 15. Manual Analyses for 315K and 315-310K Richardson Number (Ri) 0000 GMT 20 March 1982 (a) Isotachs in m/s (solid) and Montgomery Stream Function in m^2/s^2 (dashed) (b) Pressure in mb. (c) Layer Ri (solid) and Mean Layer Height in m (dashed). (d) Layer Wind Shear in m/s (solid) and Layer Thickness in m (dashed).

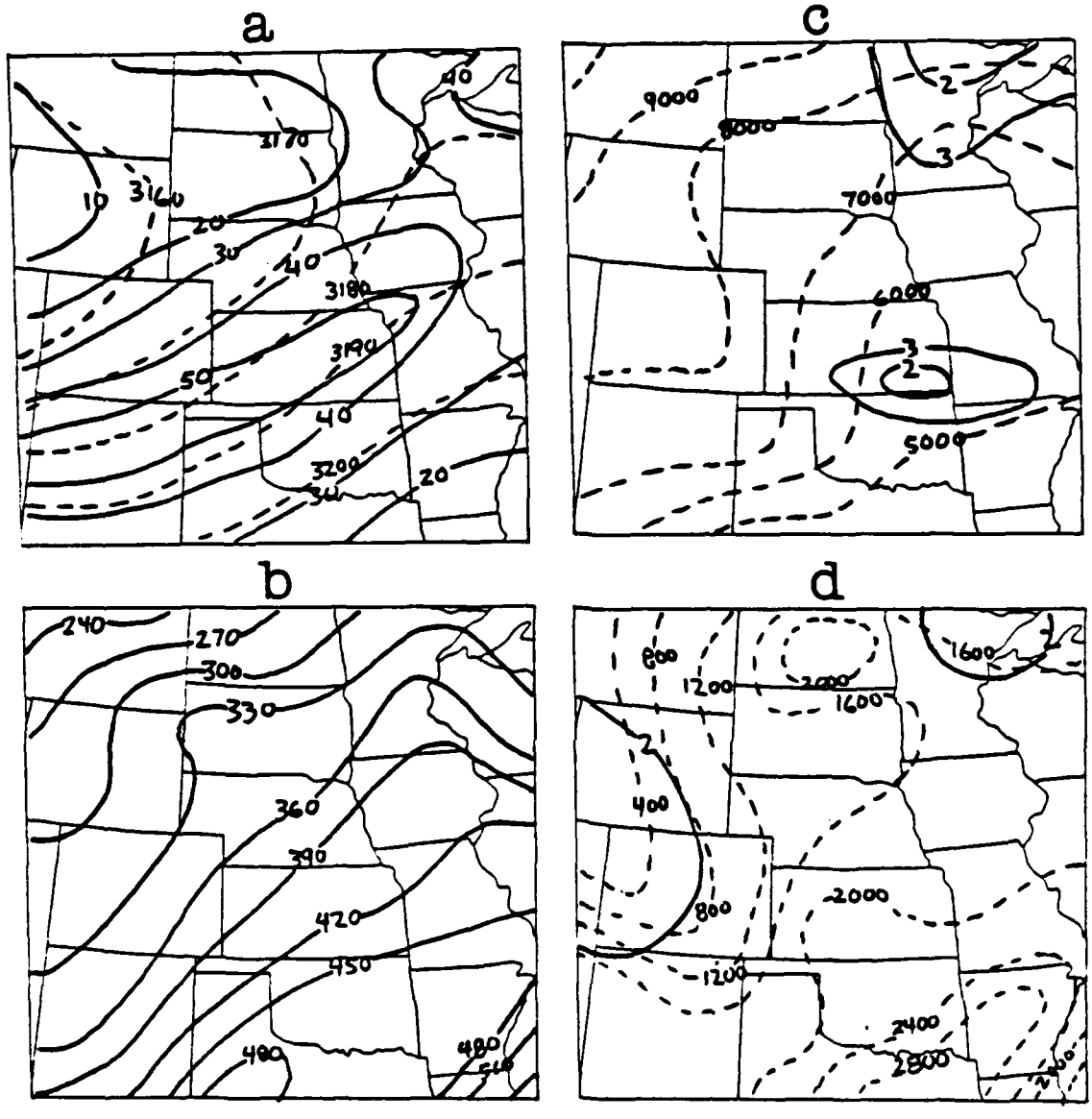

Fig. 16. Manual Analyses for 320K and 320-315K Richardson Number (Ri) 0000 GMT 20 March 1982 (a) Isotachs in m/s (solid) and Montgomery Stream Function in m^2/s^2 (dashed) (b) Pressure in mb. (c) Layer Ri (solid) and Mean Layer Height in m (dashed). (d) Layer Wind Shear in m/s (solid) and Layer Thickness in m (dashed).

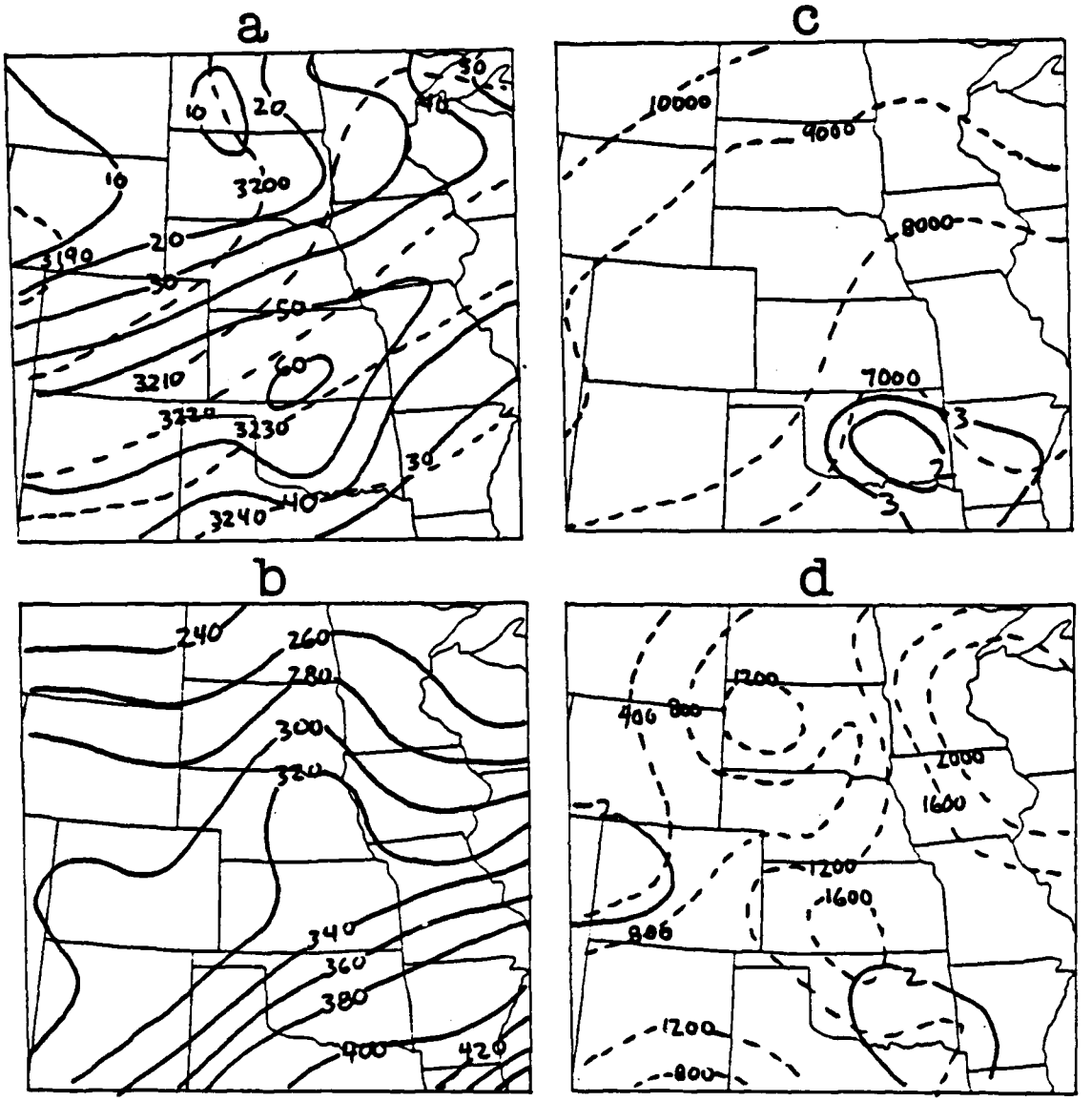

Fig. 17. Manual Analyses for 325K and 325-320K Richardson Number (Ri) 0000 GMT 20 March 1982 (a) Isotachs in m/s (solid) and Montgomery Stream Function in m^2/s^2 (dashed) (b) Pressure in mb. (c) Layer Ri (solid) and Mean Layer Height in m (dashed). (d) Layer Wind Shear in m/s (solid) and Layer Thickness in m (dashed).

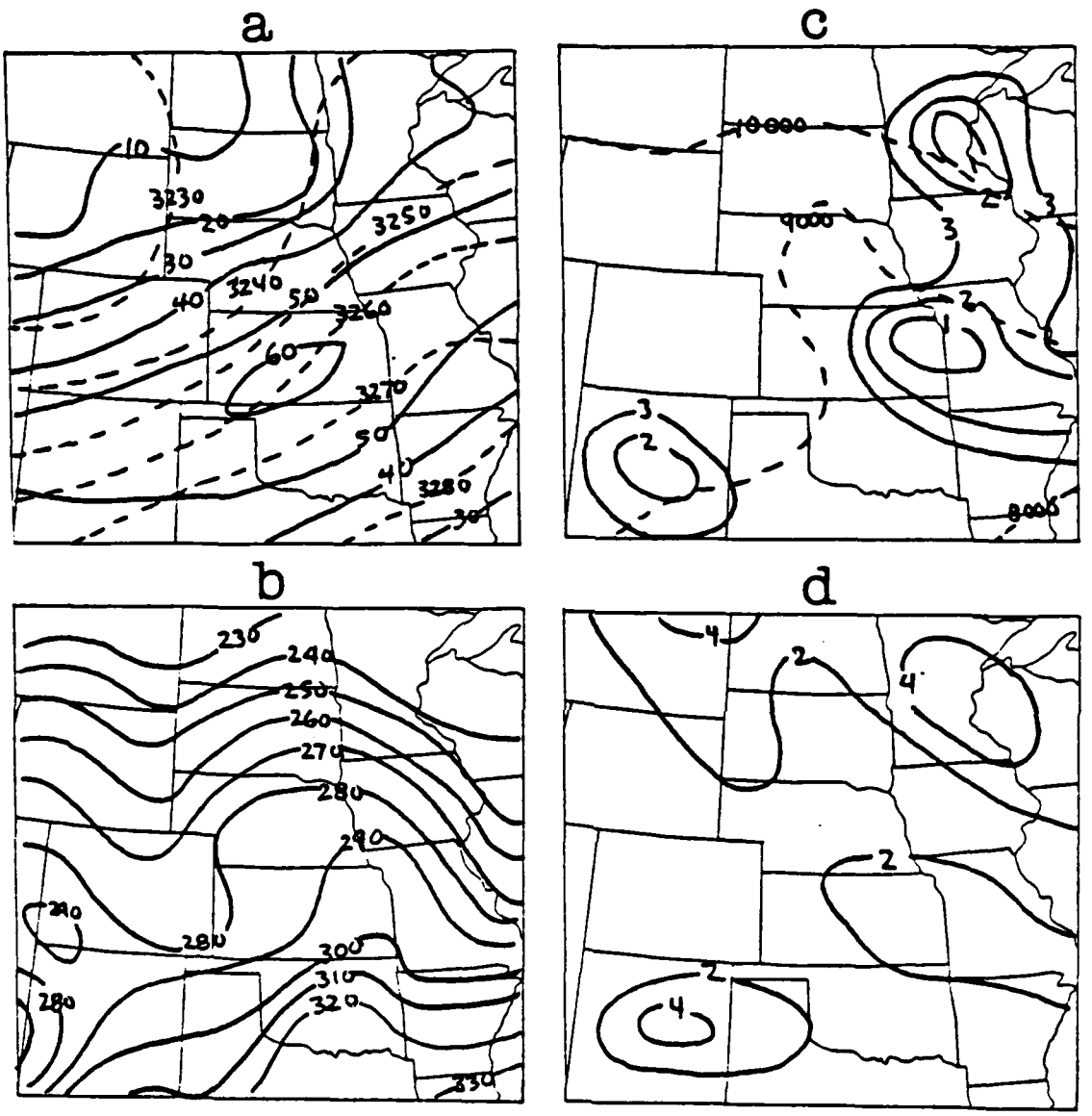

Fig. 18. Manual Analyses for 330K and 330-325K Richardson Number (Ri) 0000 GMT 20 March 1982 (a) Isotachs in m/s (solid) and Montgomery Stream Function in m^2/s^2 (dashed) (b) Pressure in mb. (c) Layer Ri (solid) and Mean Layer Height in m (dashed). (d) Layer Wind Shear in m/s (solid) and Layer Thickness in m (dashed).

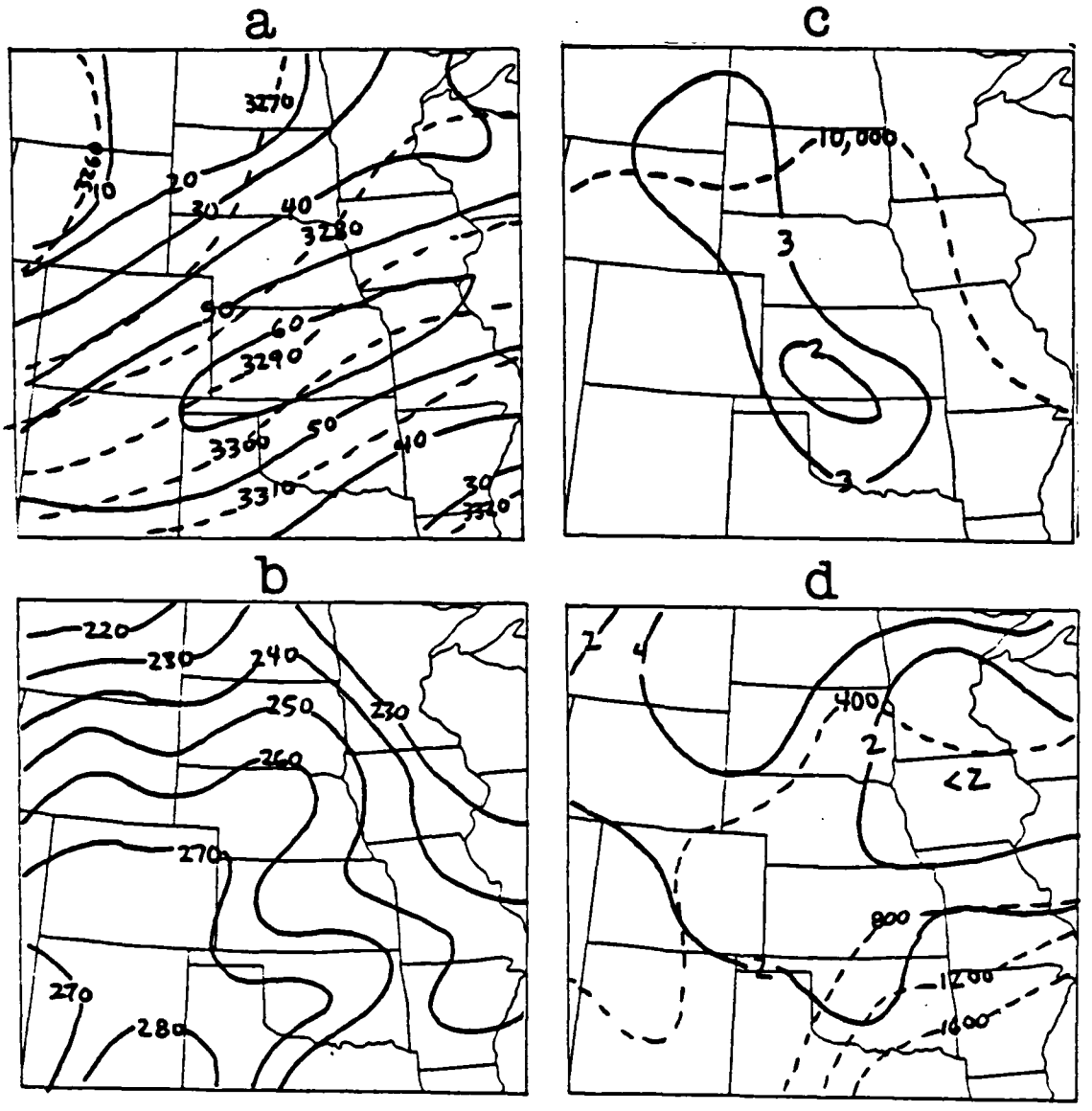

Fig. 19. Manual Analyses for 335K and 335-330K Richardson Number (Ri) 0000 GMT 20 March 1982 (a) Isotachs in m/s (solid) and Montgomery Stream Function in m^2/s^2 (dashed) (b) Pressure in mb. (c) Layer Ri (solid) and Mean Layer Height in m (dashed). (d) Layer Wind Shear in m/s (solid) and Layer Thickness in m (dashed).

REPORT #	TIME(GMT)	HEIGHT(m)	INTENSITY	Ri	SHEAR (m/s per 300m)	FIGURE USED
1	23	7,100-8,200	MDT-SVR	0.7	4.6	6
2	00	4,400	MDT	2.5	2.0	5
3	01	9,400	MDT	0.8	3.0	8
4	01	4,700	SVR	2.8	2.5	5
5	01	10,000	LGT	1.0	3.7	8
6	01	10,700	NONE	>3.0	<2.0	9
7	01	10,100	LGT	2.4	2.5	8
8	01	10,100	NONE	>3.0	<2.0	8
9	02	10,100	LGT	1.0	3.0	8
10	02	10,300	NONE	>3.0	<2.0	9
11	03	4,300	LGT-MDT	0.8	3.0	5
12	03	3,500	LGT	2.0	4.0	5
13	04	6,700	LGT-MDT	2.8	2.0	6
14	05	6,100	LGT	1.2	2.8	5
15	05	6,700-8,800	LGT-MDT	2.9	3.0	5
16	05	10,700	LGT	2.0	2.0	9
17	07	6,100	MDT-SVR	2.2	4.0	10
18	09	11,300	LGT	2.8	2.0	14
19	09	10,700	LGT	3.0	2.0	14
20	10	11,300	LGT-MDT	2.7	2.0	14
21	12	10,700	LGT-MDT	2.7	2.0	14
22	13	10,700	NONE	2.6	3.0	14
23	14	7,300-8,300	MDT	1.5	3.0	12
24	14	4,900-6,100	MDT-SVR	2.5	4.0	10
25	14	7,000	LGT-MDT	2.0	3.0	10
26	14	3,100	LGT-MDT	1.2	3.2	10
27	16	6,400	LGT	3.0	2.5	10
28	20	11,300	LGT-MDT	2.5	2.0	19
29	22	10,700	LGT	2.8	4.0	19
30	22	5,300	MDT	2.5	3.0	15

LGT = LIGHT MDT = MODERATE SVR=SEVERE

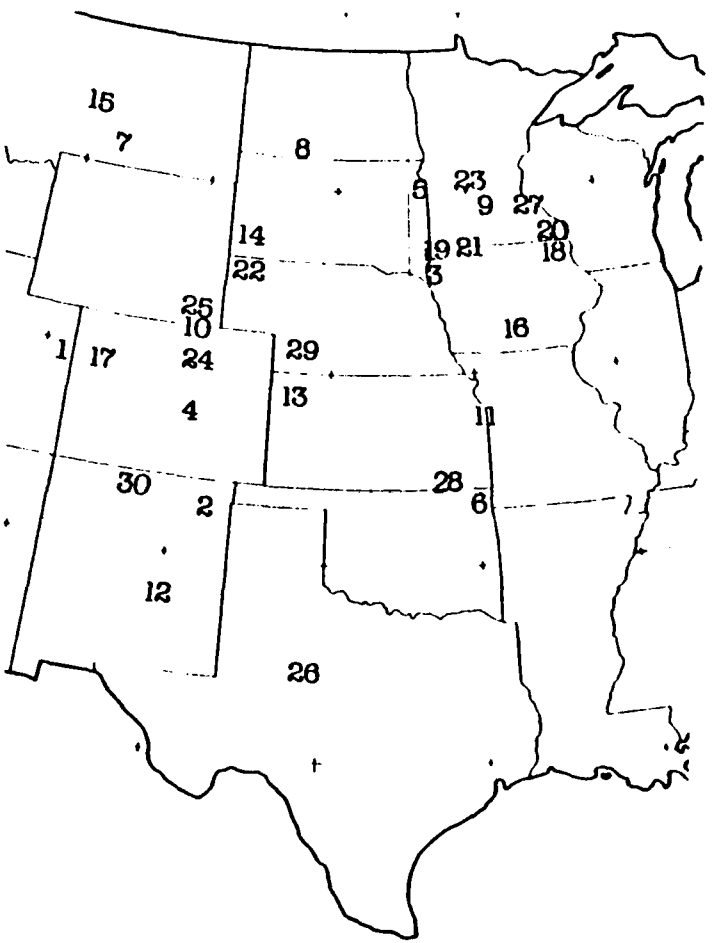

Fig. 20. Location of Clear Air Turbulence Reports.

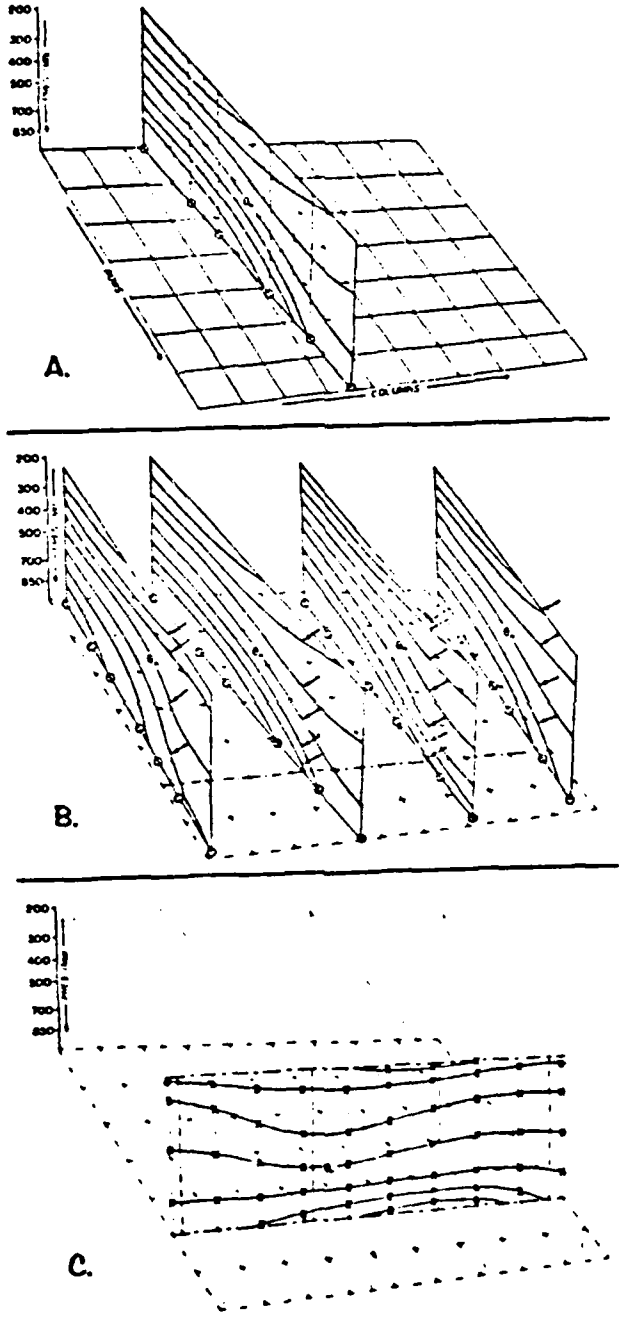

Fig. 21. Cross Section Technique Example of Three Dimensional Cross-Sectional Base of Analysis Procedure from Petersen (1986).

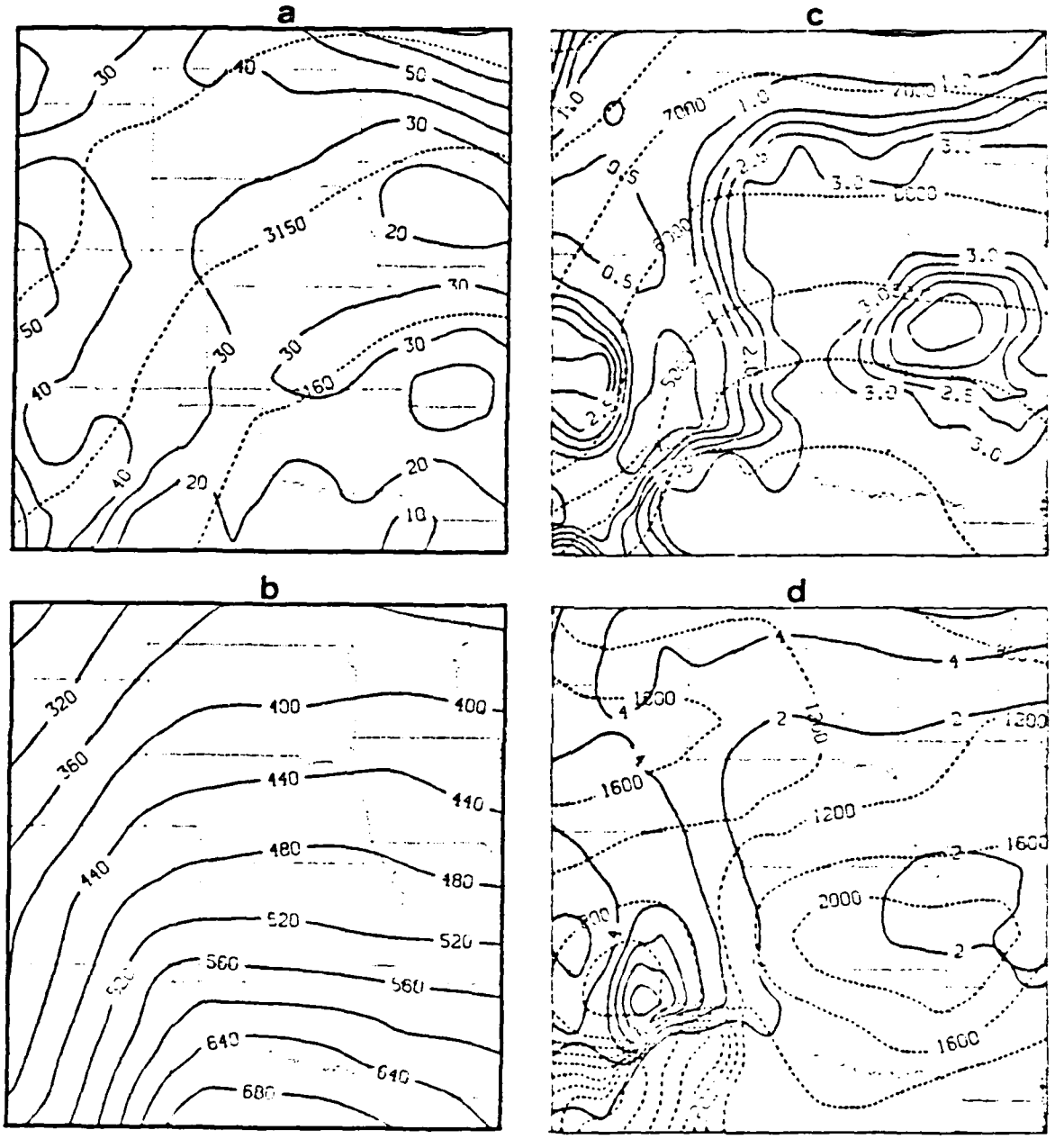

Fig. 22. Objective Analyses for 315K and 315-310K Richardson Number (Ri) 0000 GMT 19 March 1982 (a) Isotachs in m/s (solid) and Montgomery Stream Function in m^2/s^2 (dashed) (b) Pressure in mb. (c) Layer Ri (solid) and Mean Layer Height in m (dashed). (d) Layer Wind Shear in m/s (solid) and Layer Thickness in m (dashed).

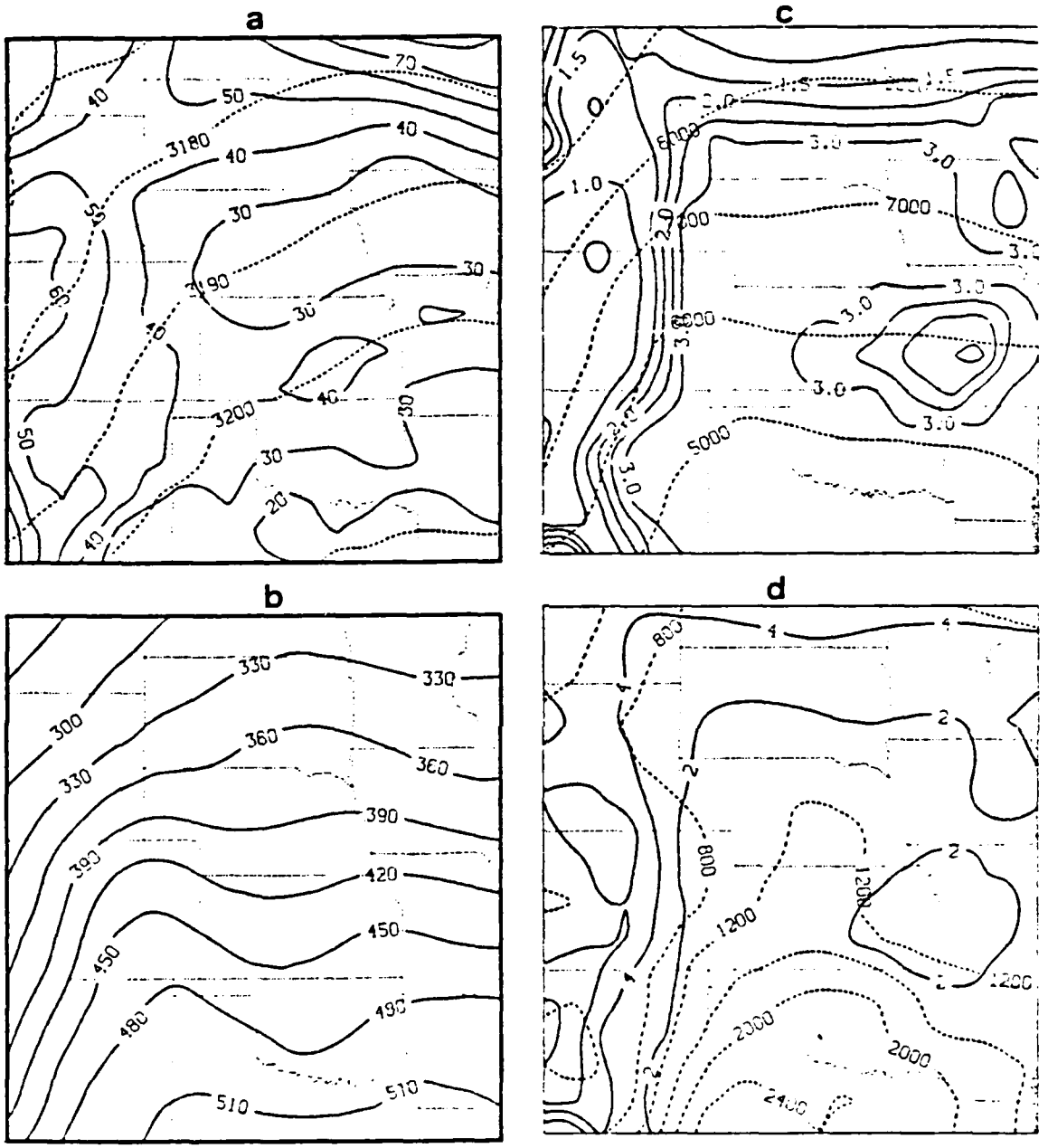

Fig. 23. Objective Analyses for 320K and 320-315K Richardson Number (Ri) 0000 GMT 19 March 1982 (a) Isotachs in m/s (solid) and Montgomery Stream Function in m^2/s^2 (dashed) (b) Pressure in mb. (c) Layer Ri (solid) and Mean Layer Height in m (dashed). (d) Layer Wind Shear in m/s (solid) and Layer Thickness in m (dashed).

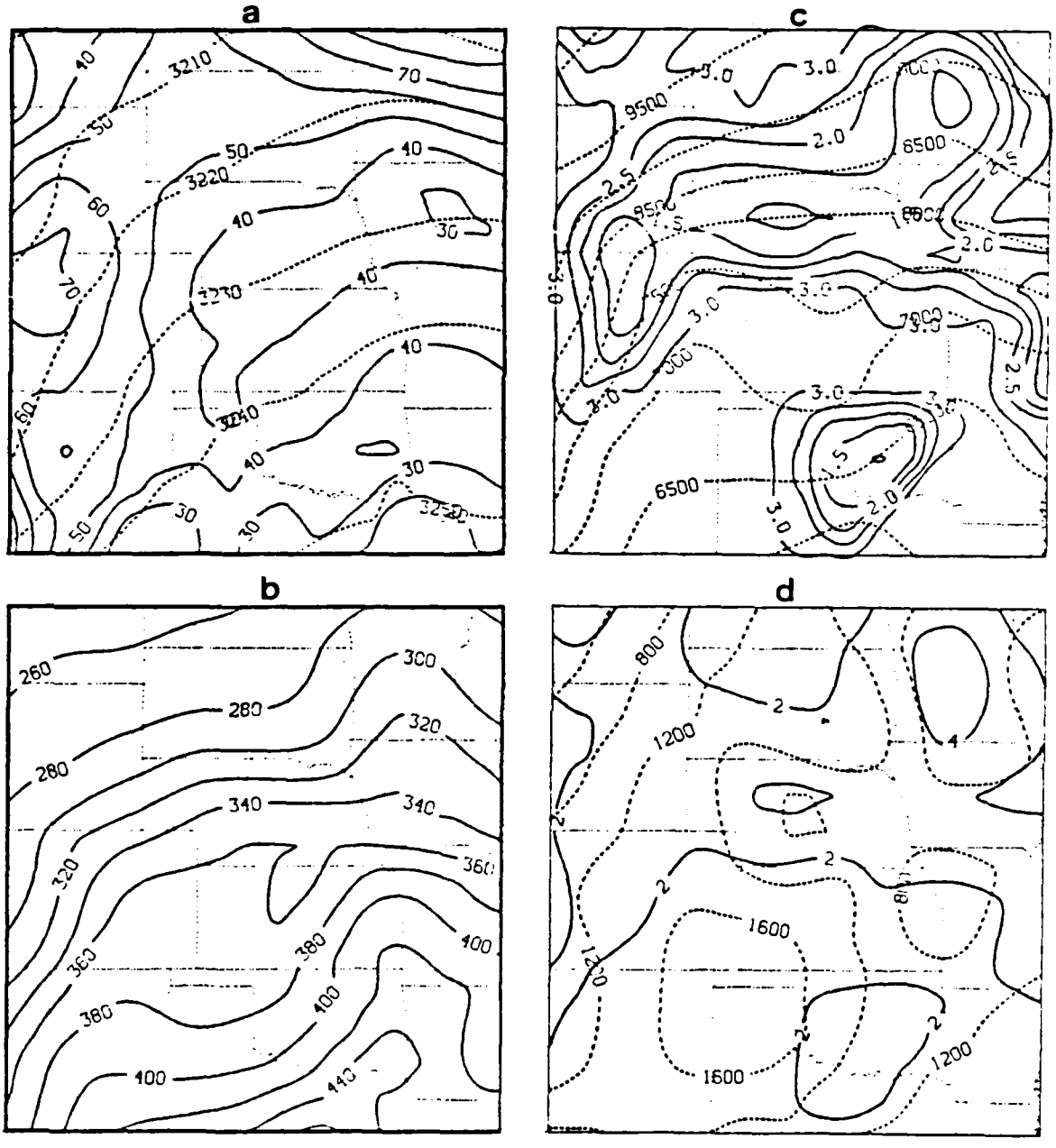

Fig. 24. Objective Analyses for 325K and 325-320K Richardson Number (Ri) 0000 GMT 19 March 1982 (a) Isotachs in m/s (solid) and Montgomery Stream Function in m^2/s^2 (dashed) (b) Pressure in mb. (c) Layer Ri (solid) and Mean Layer Height in m (dashed). (d) Layer Wind Shear in m/s (solid) and Layer Thickness in m (dashed).

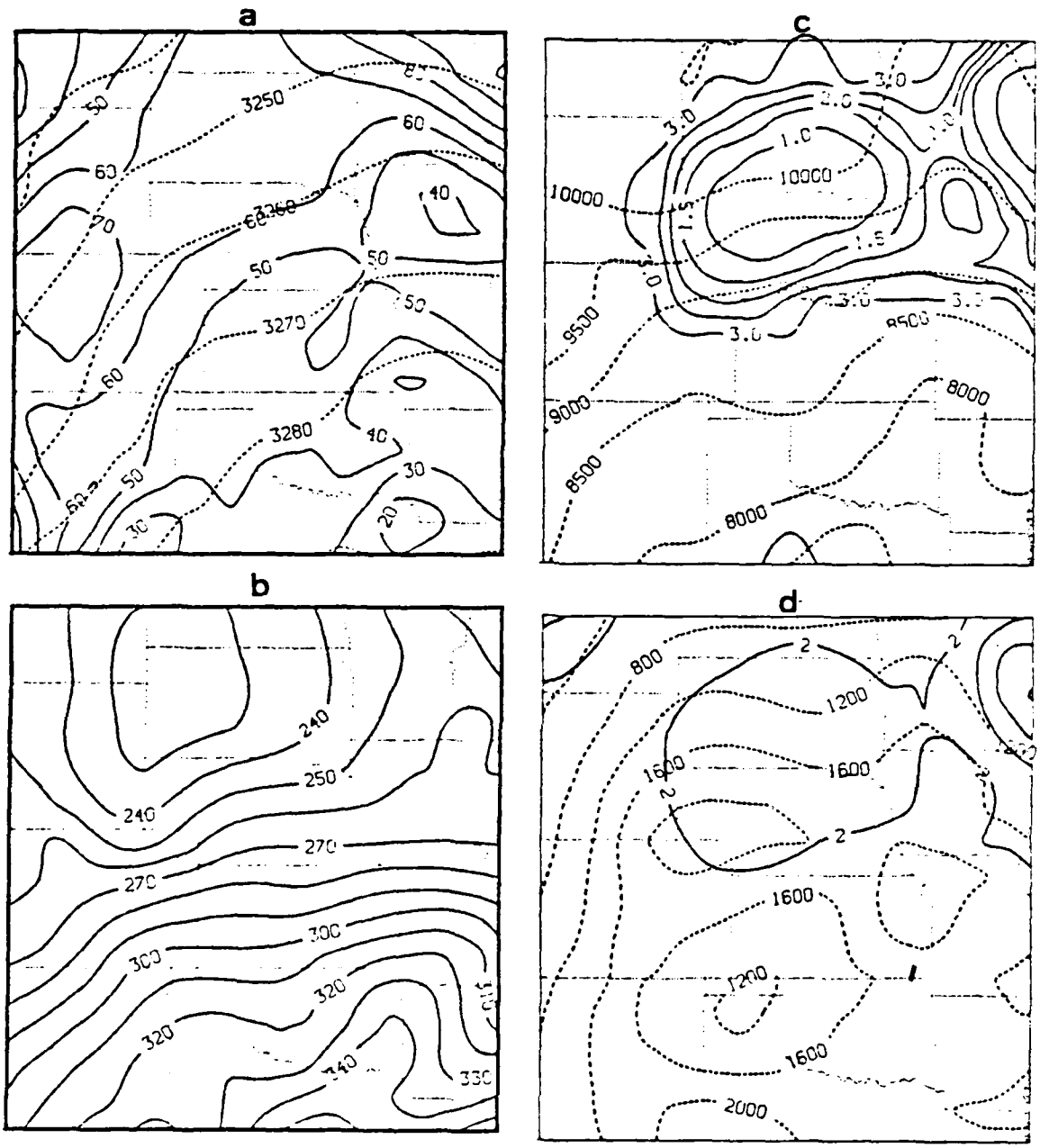

Fig. 25. Objective Analyses for 330K and 330-325K Richardson Number (Ri) 0000 GMT 19 March 1982 (a) Isotachs in m/s (solid) and Montgomery Stream Function in m^2/s^2 (dashed) (b) Pressure in mb. (c) Layer Ri (solid) and Mean Layer Height in m (dashed). (d) Layer Wind Shear in m/s (solid) and Layer Thickness in m (dashed).

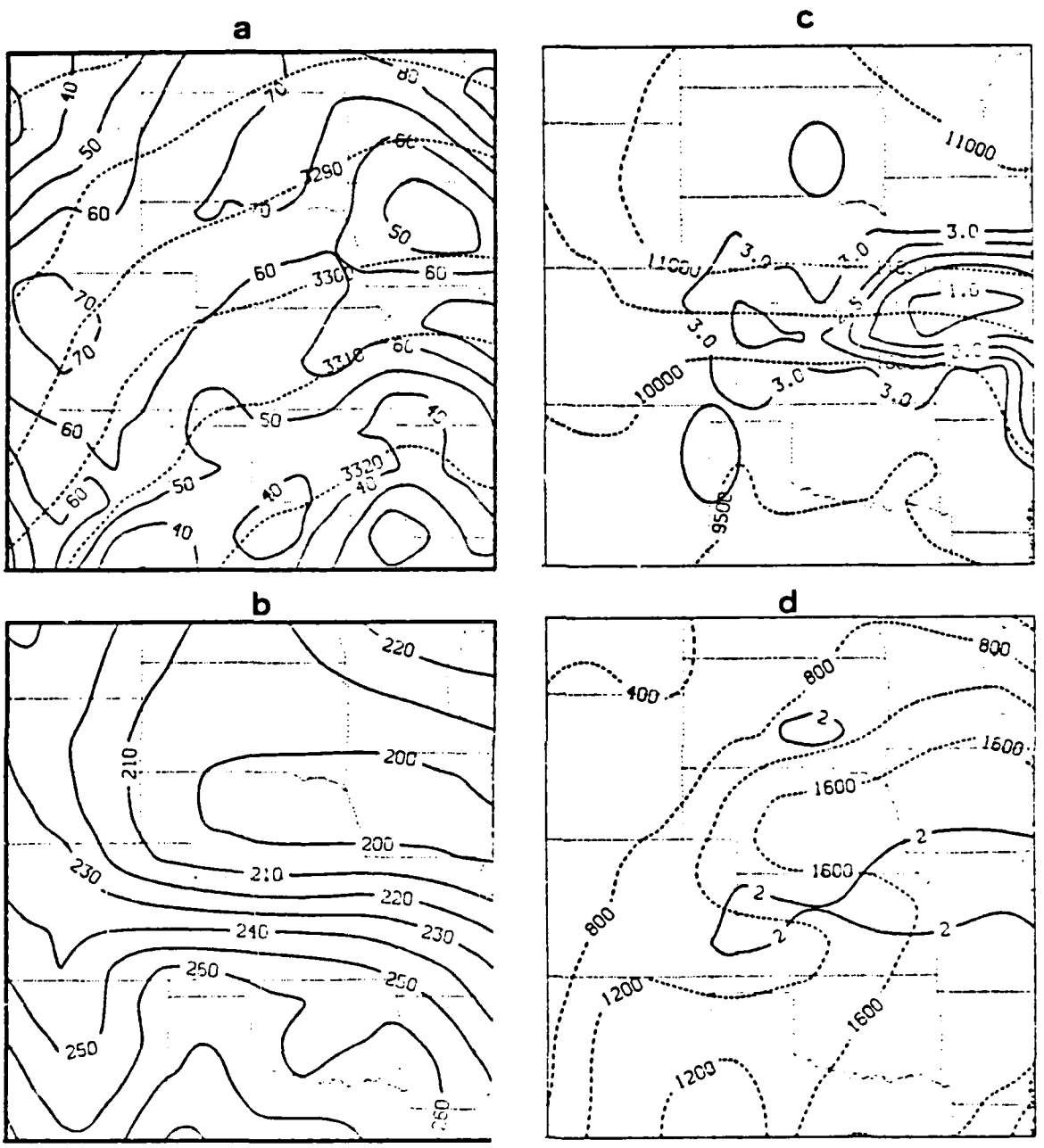

Fig. 26. Objective Analyses for 335K and 335-330K Richardson Number (Ri) 0000 GMT 19 March 1982 (a) Isotachs in m/s (solid) and Montgomery Stream Function in m^2/s^2 (dashed) (b) Pressure in mb. (c) Layer Ri (solid) and Mean Layer Height in m (dashed). (d) Layer Wind Shear in m/s (solid) and Layer Thickness in m (dashed).

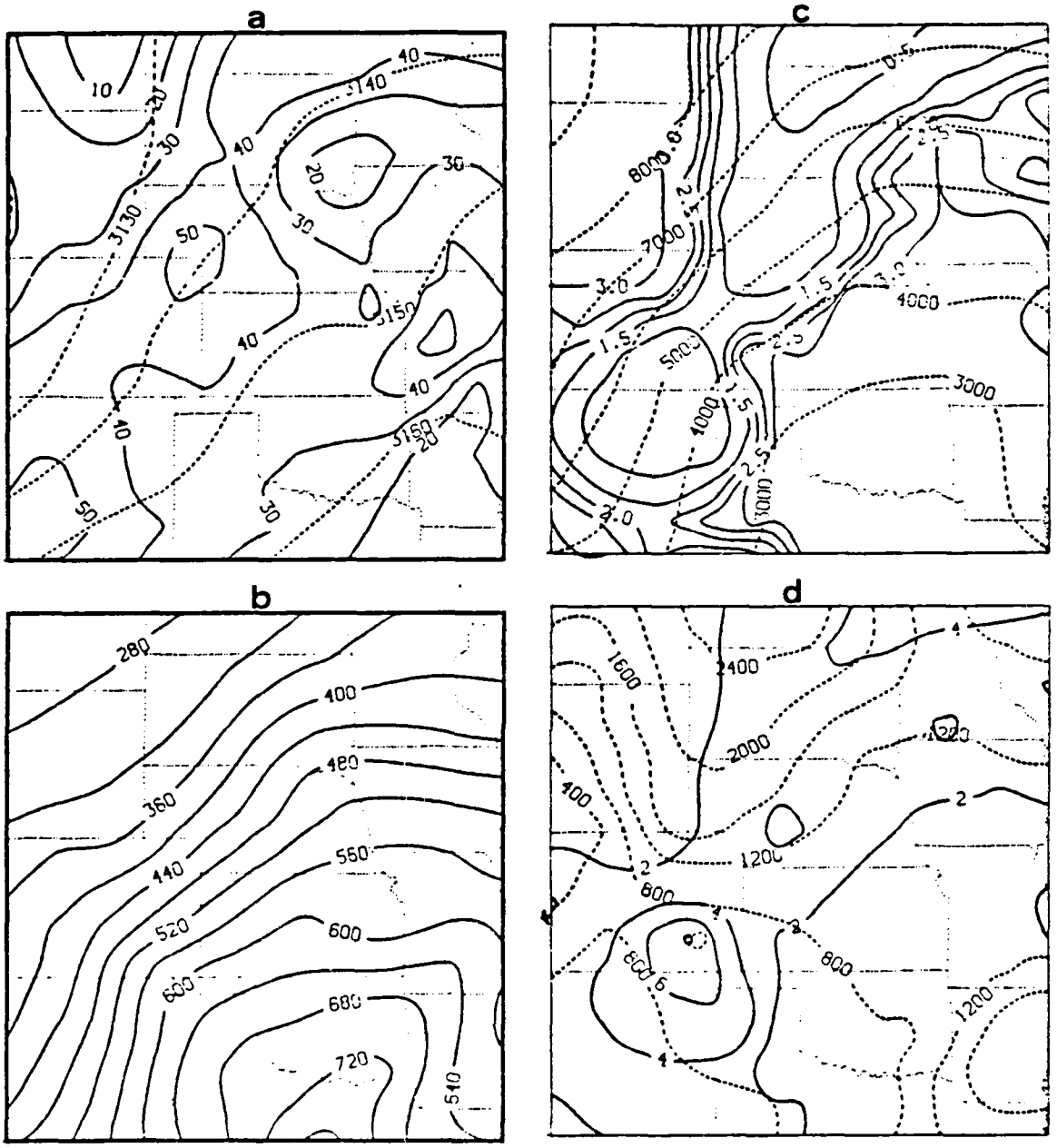

Fig. 27. Objective Analyses for 315K and 315-310K Richardson Number (Ri) 1200 GMT 19 March 1982 (a) Isotachs in m/s (solid) and Montgomery Stream Function in m^2/s^2 (dashed) (b) Pressure in mb. (c) Layer Ri (solid) and Mean Layer Height in m (dashed). (d) Layer Wind Shear in m/s (solid) and Layer Thickness in m (dashed).

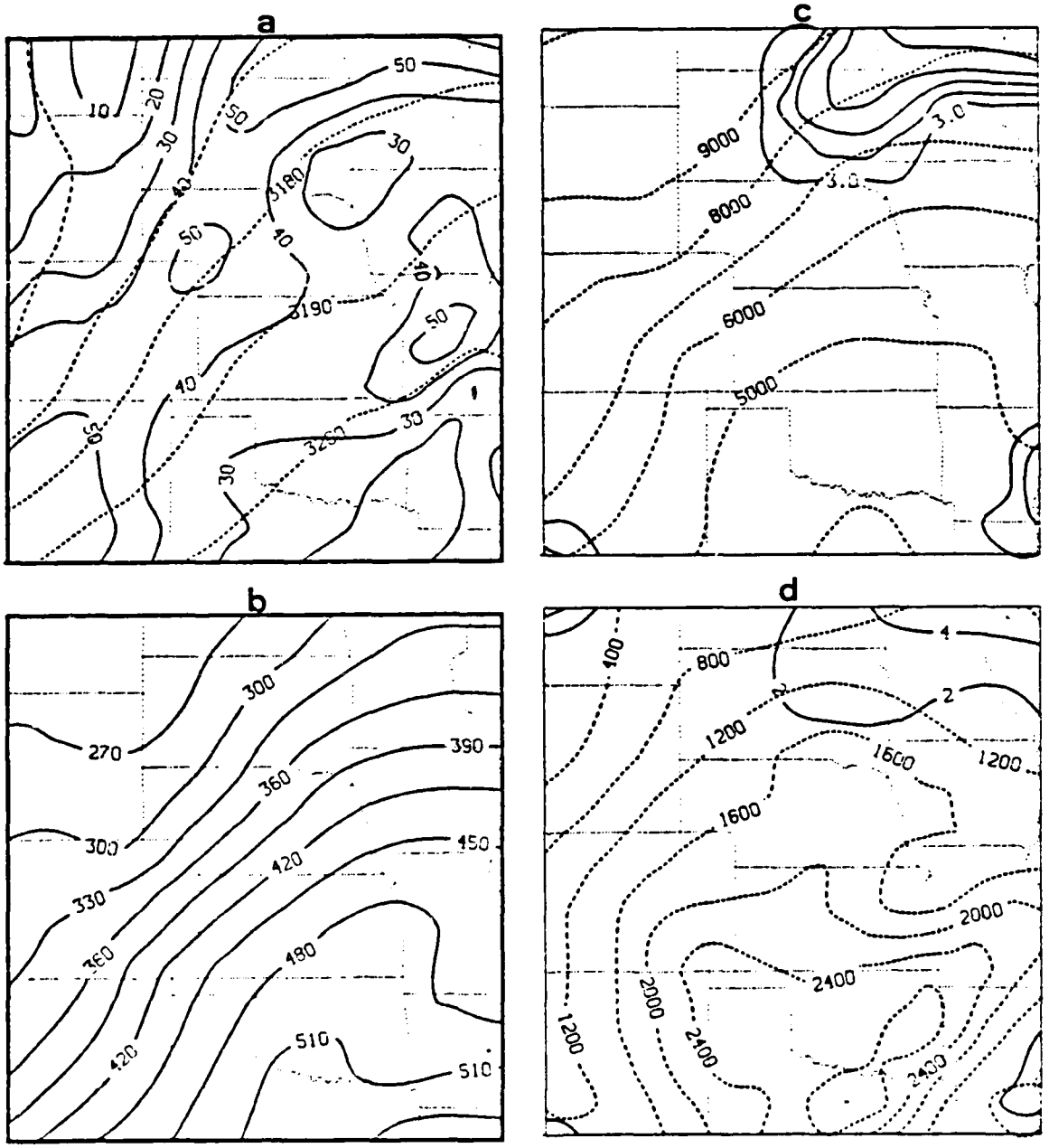

Fig. 28. Objective Analyses for 320K and 320-315K Richardson Number (Ri) 1200 GMT 19 March 1982 (a) Isotachs in m/s (solid) and Montgomery Stream Function in m^2/s^2 (dashed) (b) Pressure in mb. (c) Layer Ri (solid) and Mean Layer Height in m (dashed). (d) Layer Wind Shear in m/s (solid) and Layer Thickness in m (dashed).

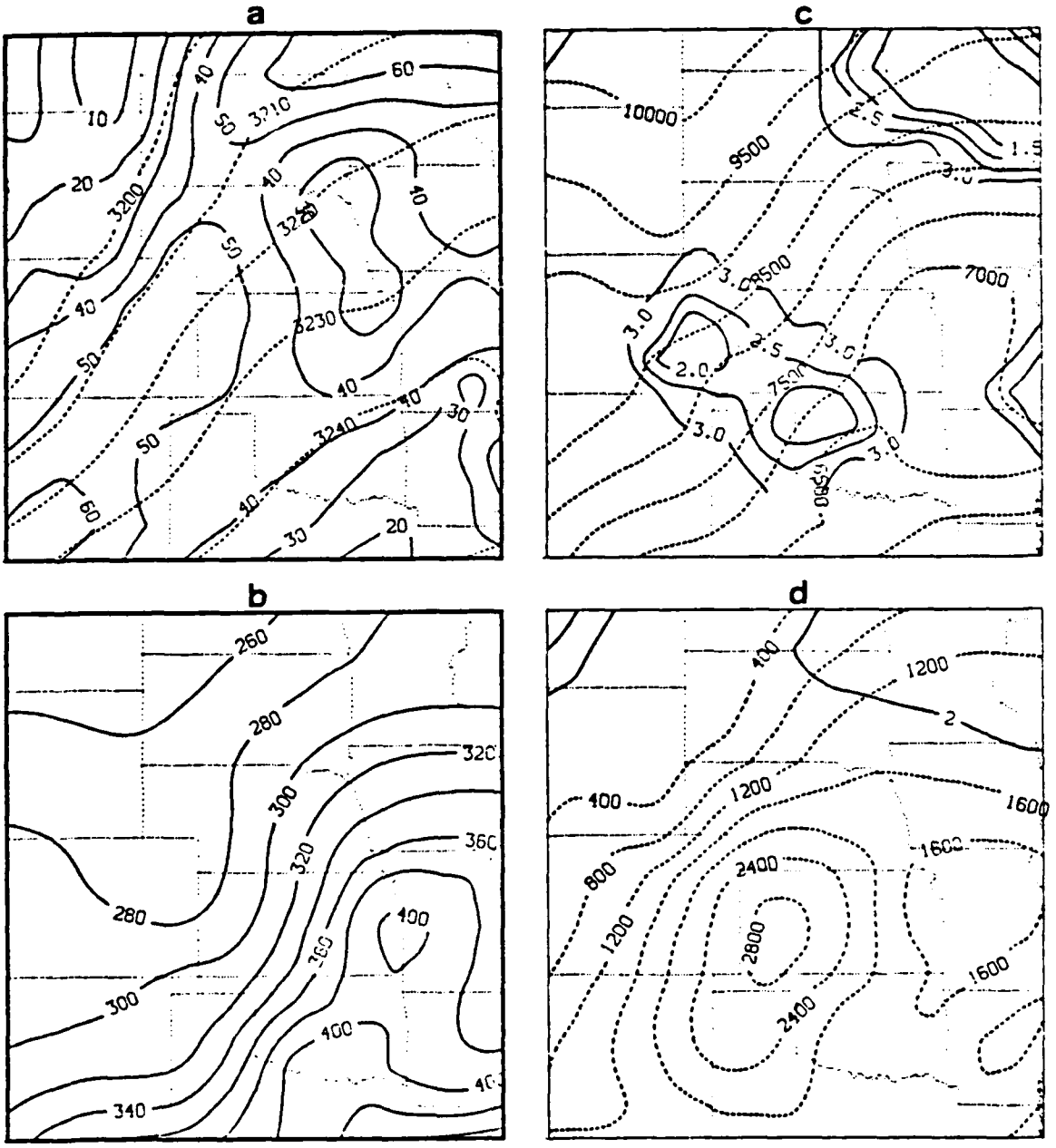

Fig. 29. Objective Analyses for 325K and 325-320K Richardson Number (Ri) 1200 GMT 19 March 1982 (a) Isotachs in m/s (solid) and Montgomery Stream Function in m^2/s^2 (dashed) (b) Pressure in mb. (c) Layer Ri (solid) and Mean Layer Height in m (dashed). (d) Layer Wind Shear in m/s (solid) and Layer Thickness in m (dashed).

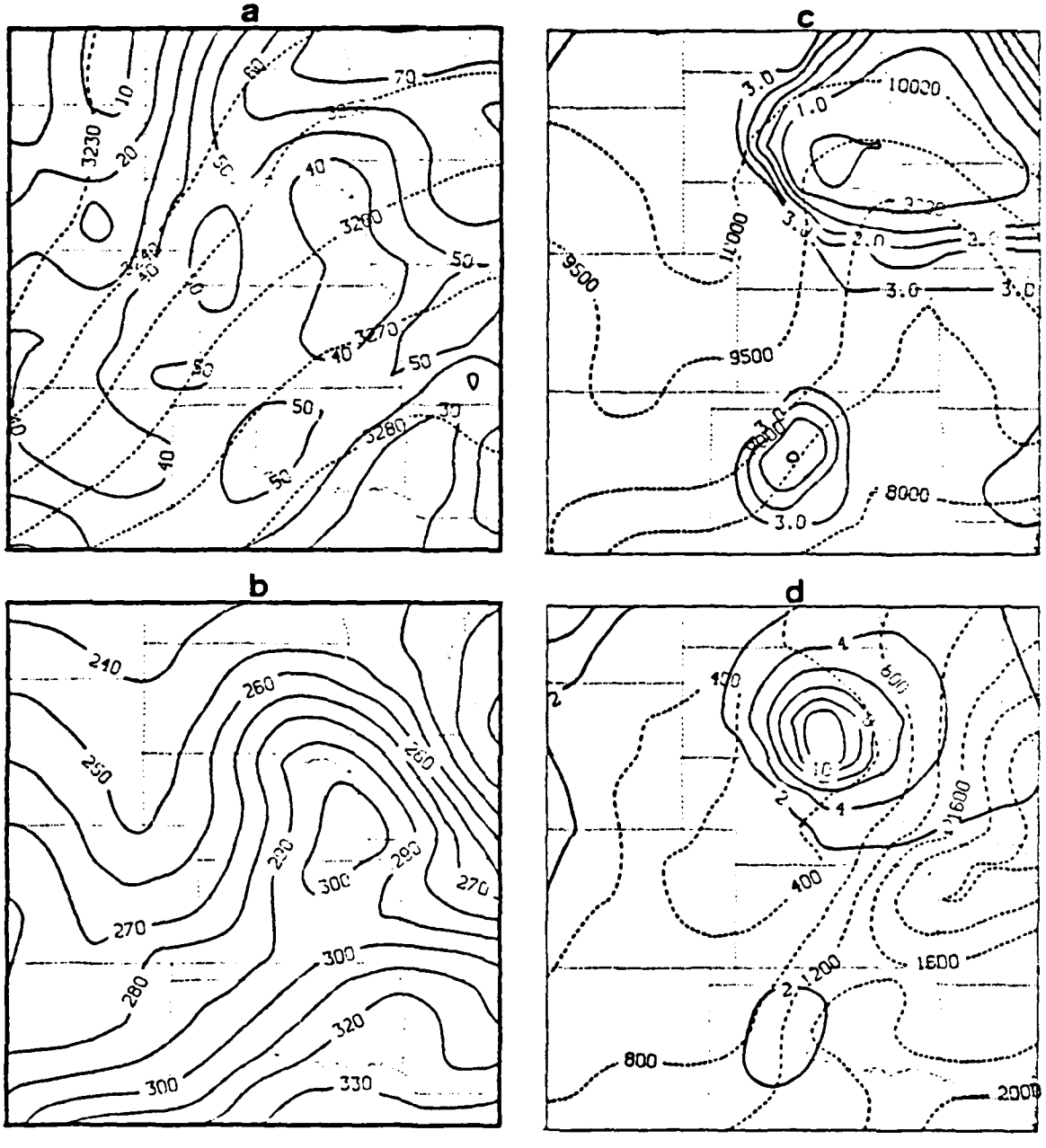

Fig. 30. Objective Analyses for 330K and 330-325K Richardson Number (Ri) 1200 GMT 19 March 1982 (a) Isotachs in m/s (solid) and Montgomery Stream Function in m^2/s^2 (dashed) (b) Pressure in mb. (c) Layer Ri (solid) and Mean Layer Height in m (dashed). (d) Layer Wind Shear in m/s (solid) and Layer Thickness in m (dashed).

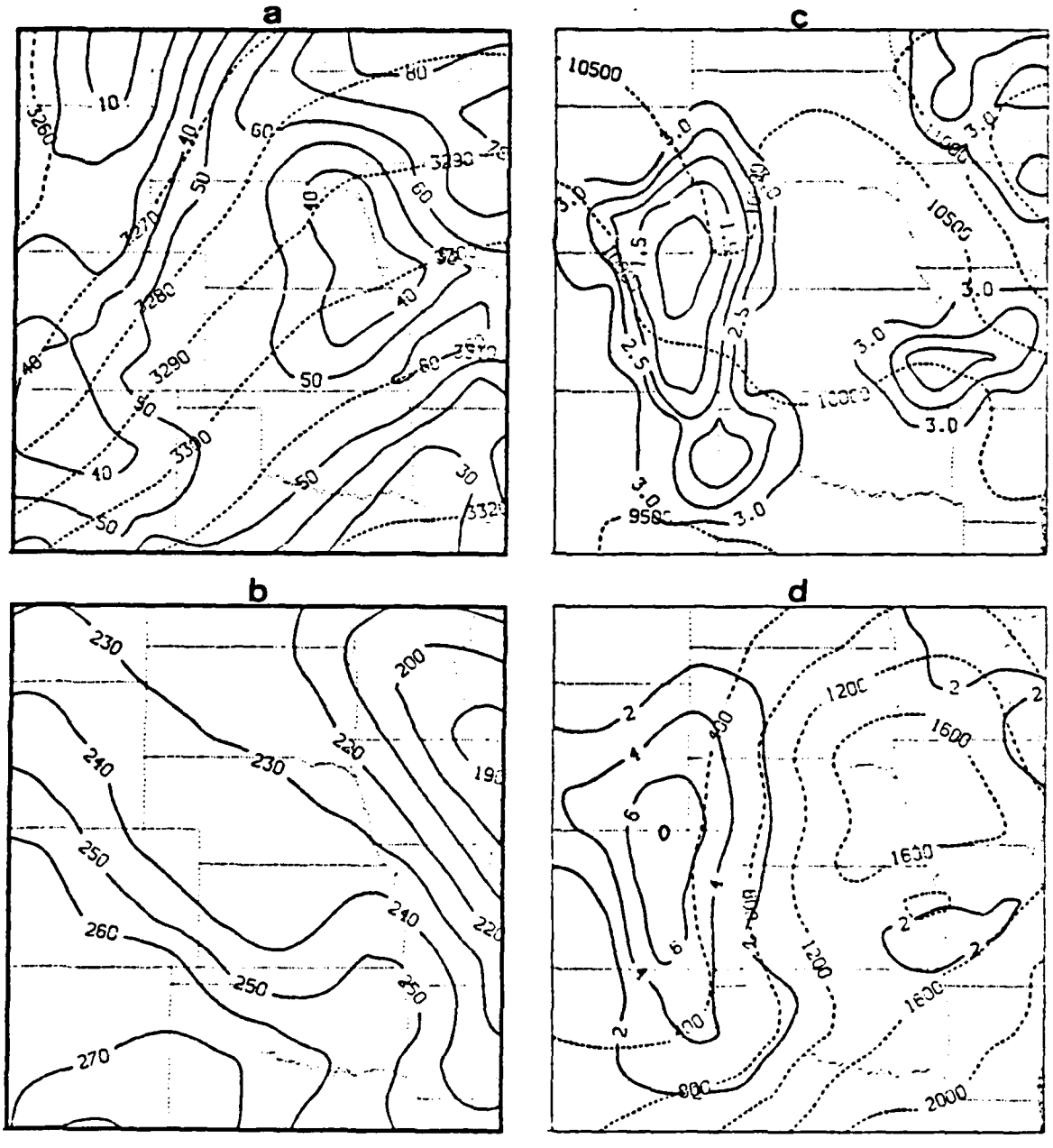

Fig. 31. Objective Analyses for 335K and 335-330K Richardson Number (Ri) 1200 GMT 19 March 1982 (a) Isotachs in m/s (solid) and Montgomery Stream Function in m^2/s^2 (dashed) (b) Pressure in mb. (c) Layer Ri (solid) and Mean Layer Height in m (dashed). (d) Layer Wind Shear in m/s (solid) and Layer Thickness in m (dashed).

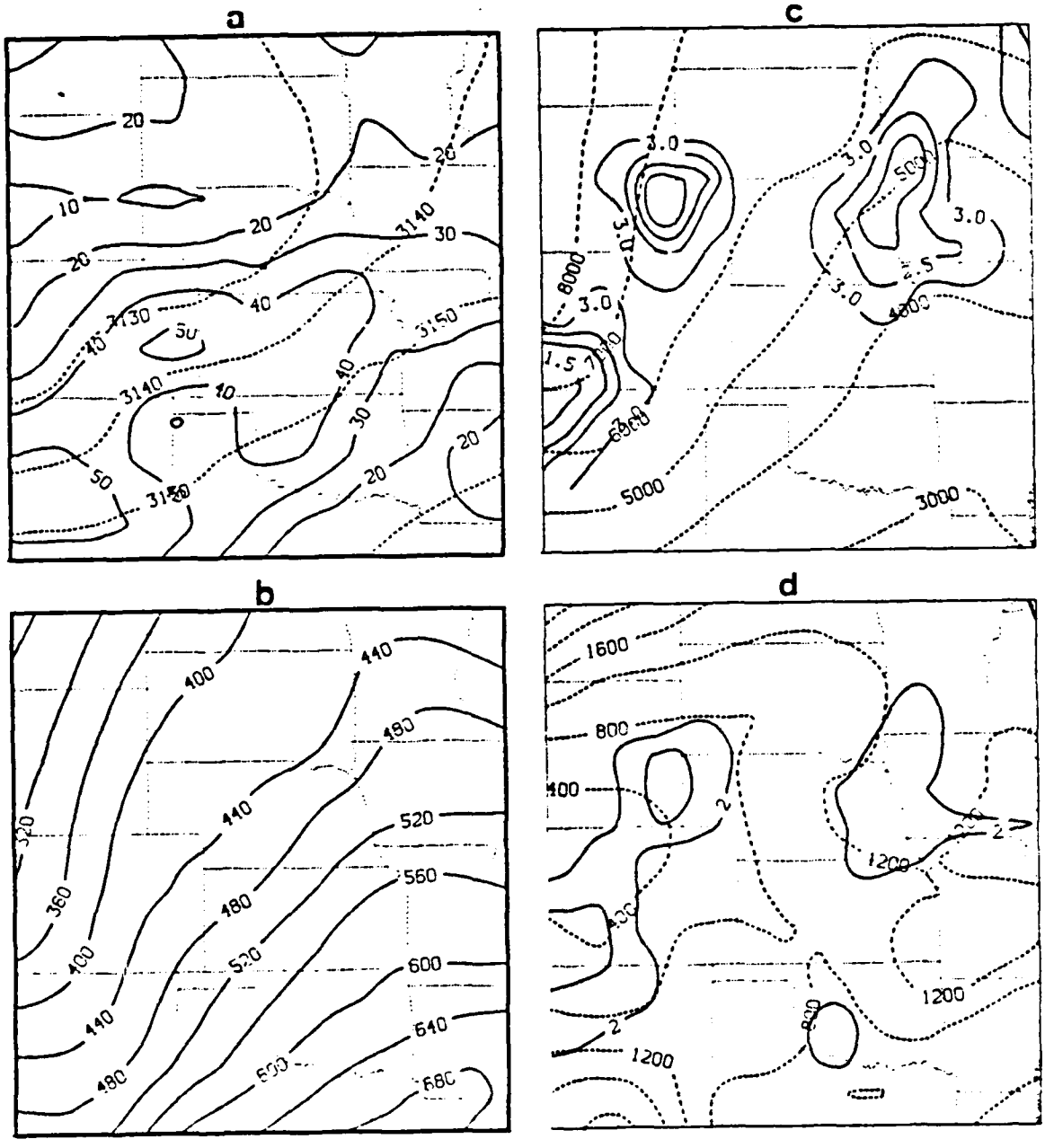

Fig. 32. Objective Analyses for 315K and 315-310K Richardson Number (Ri) 0000 GMT 20 March 1982 (a) Isotachs in m/s (solid) and Montgomery Stream Function in m^2/s^2 (dashed) (b) Preasure in mb. (c) Layer Ri (solid) and Mean Layer Height in m (dashed). (d) Layer Wind Shear in m/s (solid) and Layer Thickness in m (dashed).

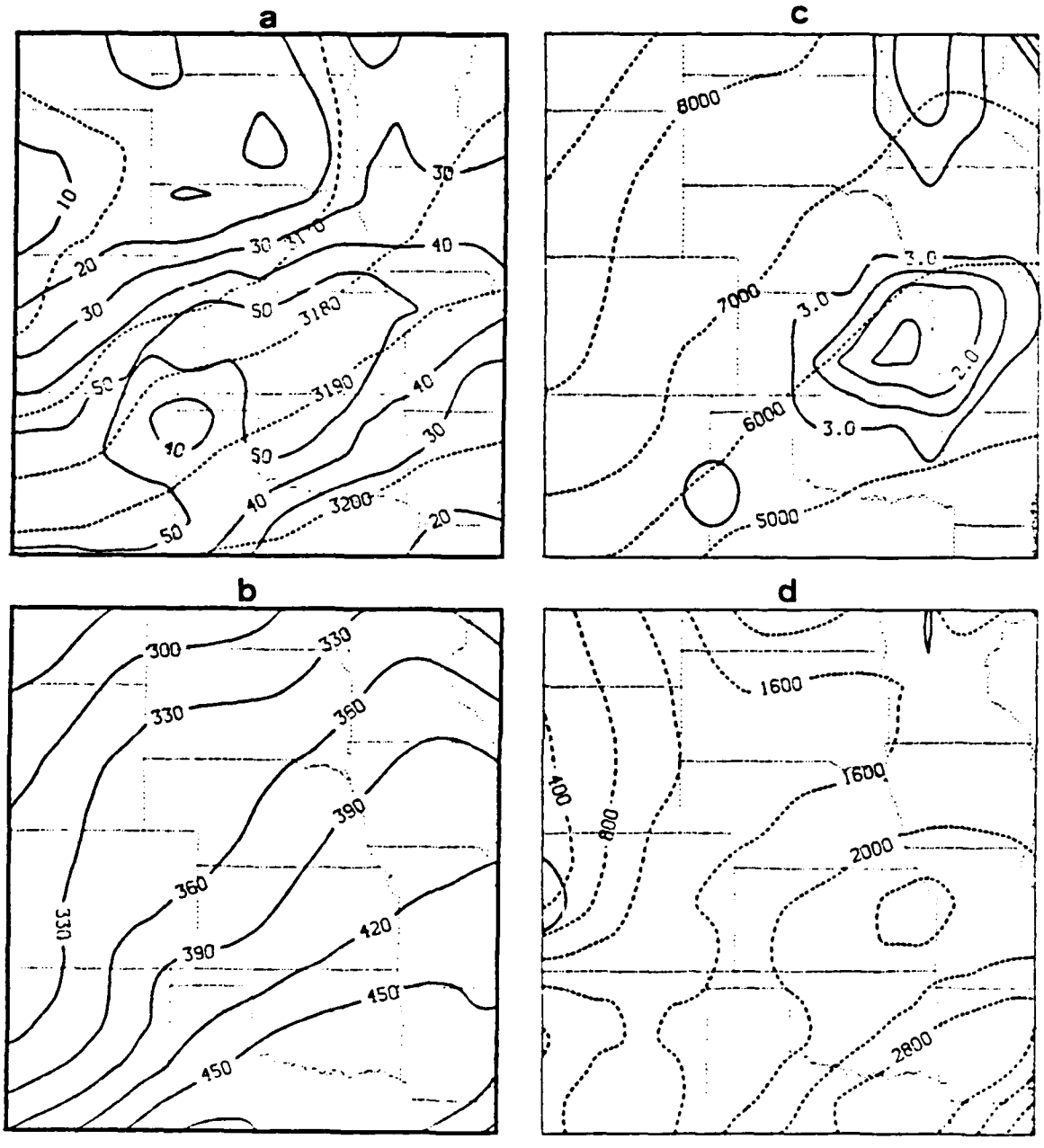

Fig. 33. Objective Analyses for 320K and 320-315K Richardson Number (Ri) 0000 GMT 20 March 1982 (a) Isotachs in m/s (solid) and Montgomery Stream Function in m^2/s^2 (dashed) (b) Pressure in mb. (c) Layer Ri (solid) and Mean Layer Height in m (dashed). (d) Layer Wind Shear in m/s (solid) and Layer Thickness in m (dashed).

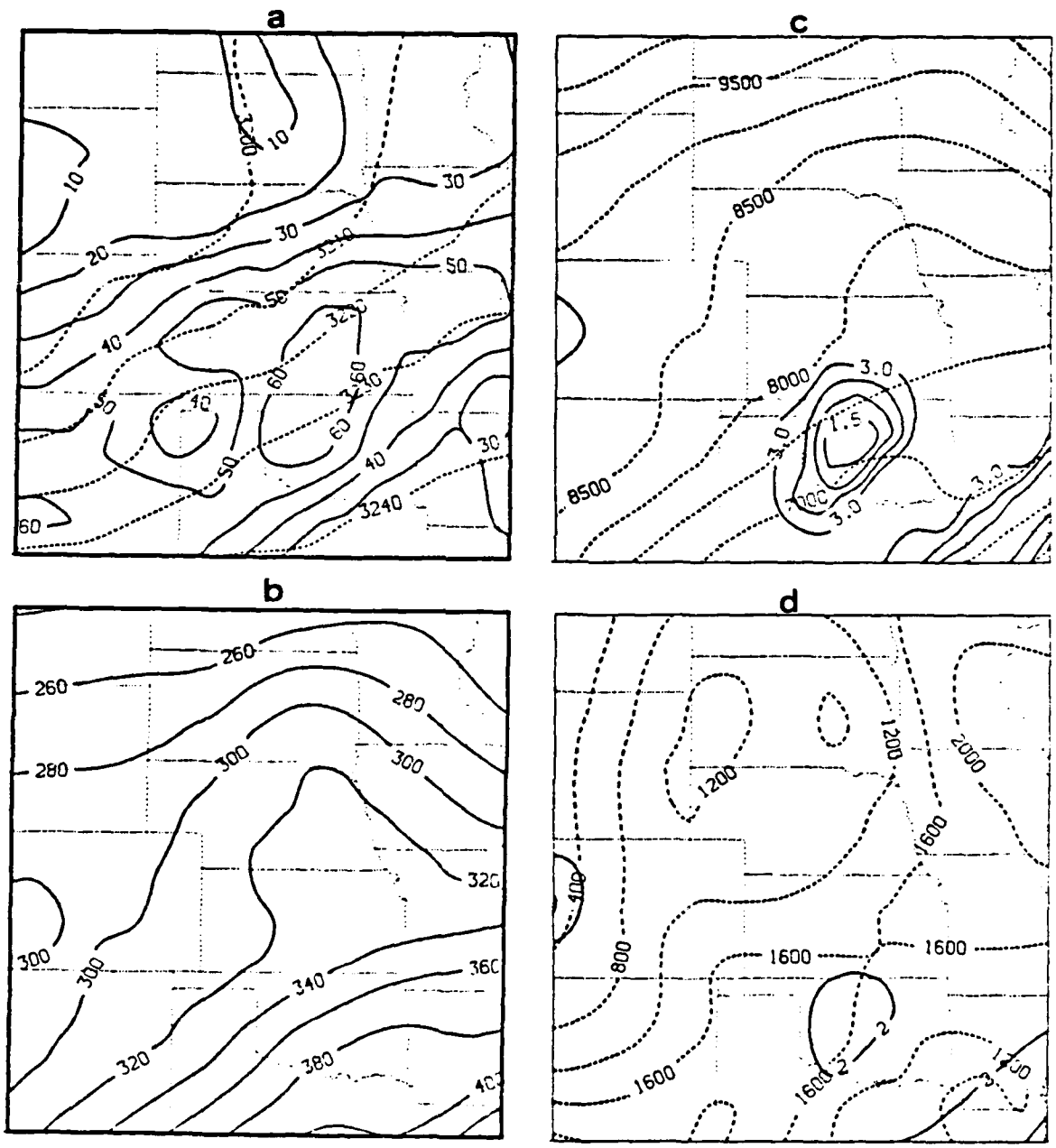

Fig. 34. Objective Analyses for 325K and 325-320K Richardson Number (Ri) 0000 GMT 20 March 1982 (a) Isotachs in m/s (solid) and Montgomery Stream Function in m^2/s^2 (dashed) (b) Pressure in mb. (c) Layer Ri (solid) and Mean Layer Height in m (dashed). (d) Layer Wind Shear in m/s (solid) and Layer Thickness in m (dashed).

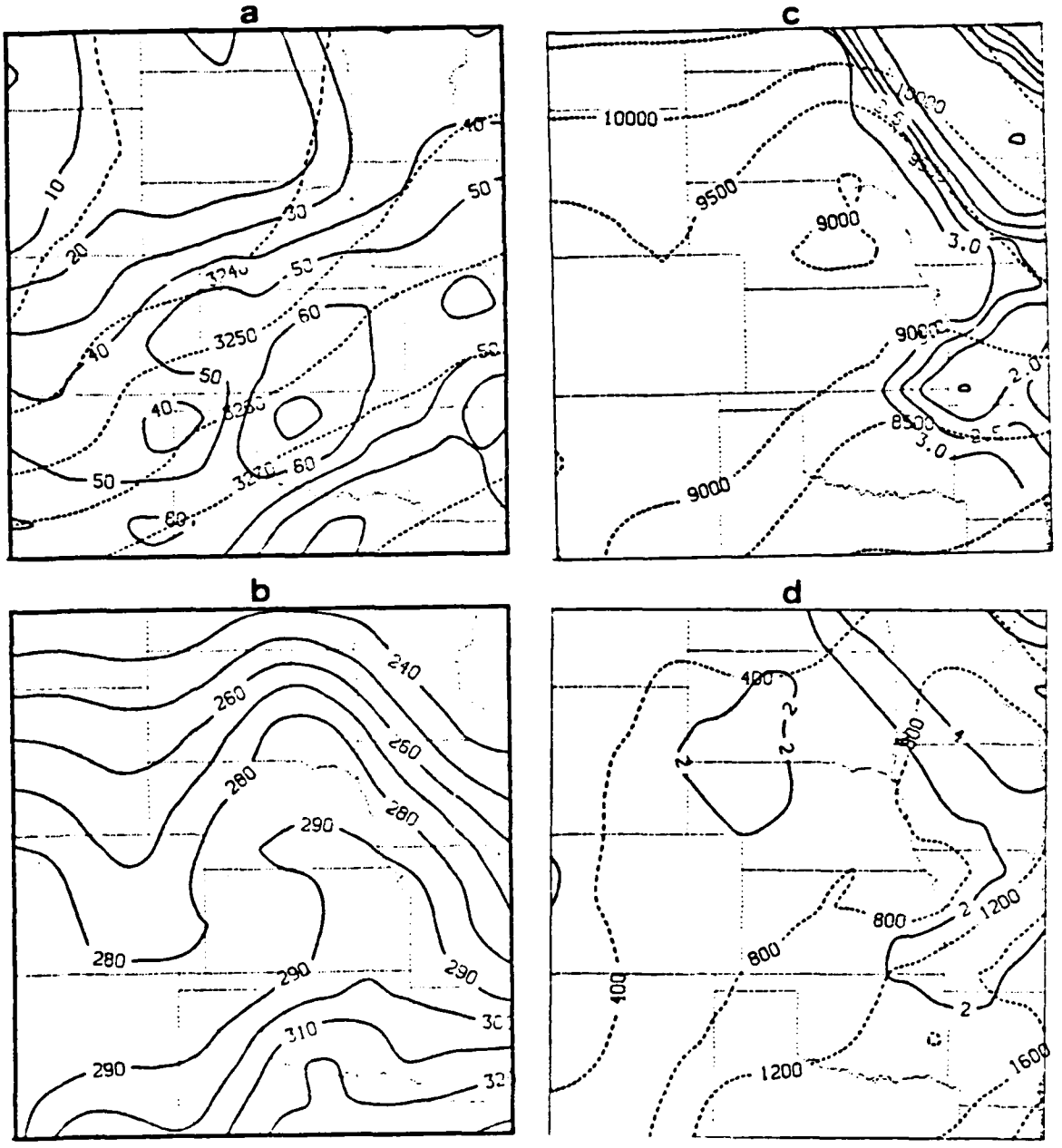

Fig. 35. Objective Analyses for 330K and 330-325K Richardson Number (Ri) 0000 GMT 20 March 1982 (a) Isotachs in m/s (solid) and Montgomery Stream Function in m^2/s^2 (dashed) (b) Pressure in mb. (c) Layer Ri (solid) and Mean Layer Height in m (dashed). (d) Layer Wind Shear in m/s (solid) and Layer Thickness in m (dashed).

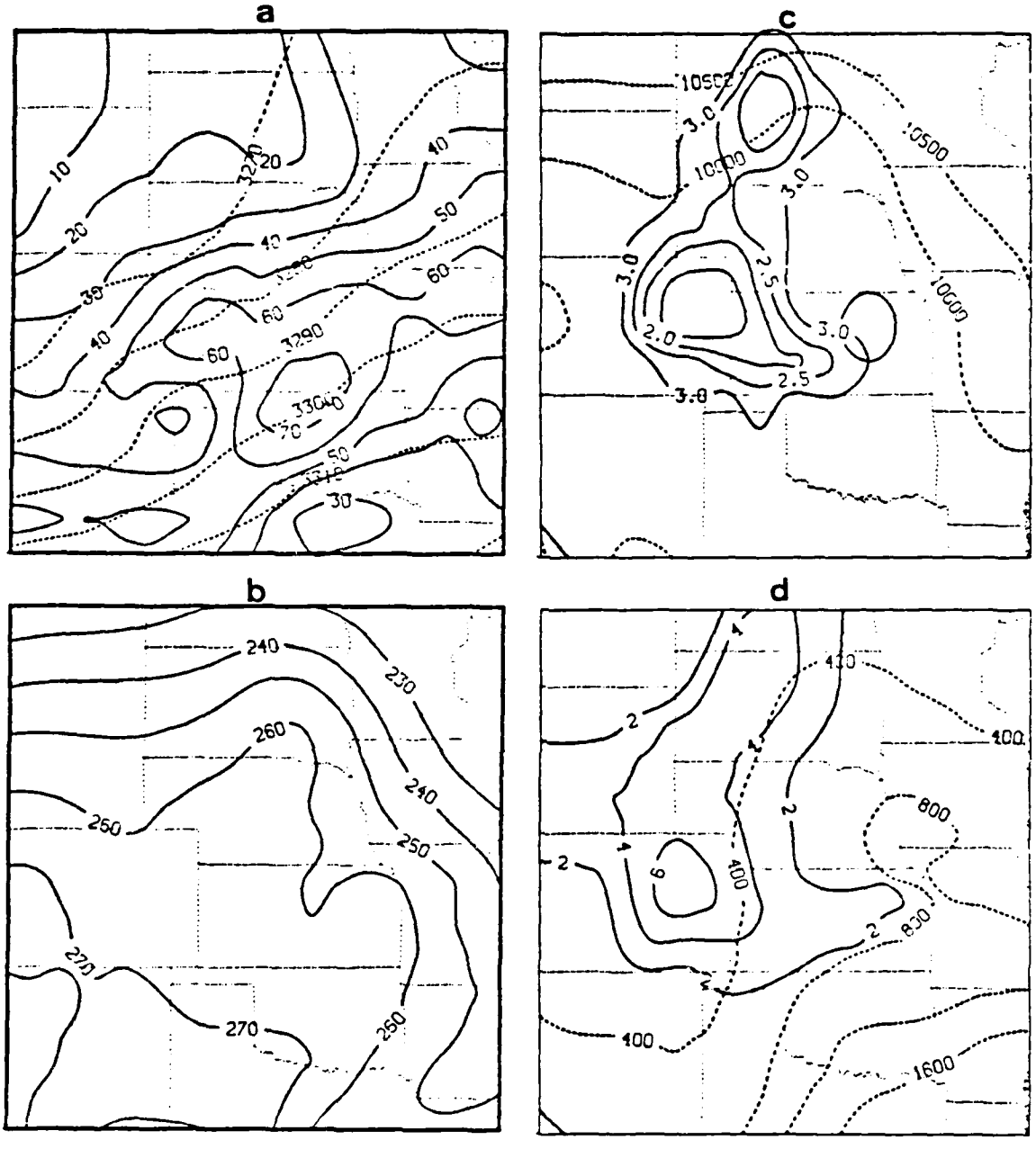

Fig. 36. Objective Analyses for 335K and 335-330K Richardson Number (Ri) 0000 GMT 20 March 1982 (a) Isotachs in m/s (solid) and Montgomery Stream Function in m^2/s^2 (dashed) (b) Pressure in mb. (c) Layer Ri (solid) and Mean Layer Height in m (dashed). (d) Layer Wind Shear in m/s (solid) and Layer Thickness in m (dashed).

TABLE 1

FREQUENCY(%) OF TURBULENCE IN DIFFERENT GEOGRAPHICAL REGIONS

(AFTER VINNICHENKO, 1980)

Intensity	Canada, Greenland	USA	Atlantic 25-40N	Atlantic 45-70N	Western Europe	USSR	Japan
None	84.0	69.0	81.0	88.0	92.0	88.3	53.3
Light	10.4	21.3	12.0	7.5	5.0	5.7	34.5
Moderate	5.2	9.3	7.0	4.3	2.8	5.6	11.8
Severe	0.4	0.4	0.0	0.2	0.3	0.4	0.6
Extreme	-	-	-	-	-	-	-

LIST OF REFERENCES

Atlas, D. and K. R. Hardy, 1966: Optimizing the radar detection of clear air turbulence. J. Appl. Meteor. 5, 450-460.

Boucher, R. J., 1974: Evaluation of Clear Air Turbulence Detection by Ground-Based Radars, Special Rawinsondes, and Aircraft, 1967-1971. AFCRL-TR-74-0489, Bedford, Mass., 104pp.

Browning, K. A., 1971: Structure of the atmosphere in the vicinity of large-amplitude Kelvin-Helmholtz billows, Quart. J. R. Met. Soc., 97, 283-299.

Dutton, J. A. and H. A. Panofsky, 1970: Clear air turbulence: a mystery may be unfolding. Science, 20, 937-944.

Hicks, J. J., 1969: Radar observations of a gravatational wave in clear air near the tropopause associated with CAT. J. Appl. Meteor., 8, 627-633.

Hopkins R. H., 1977: Forecasting Techniques of Clear Air Turbulence Including That Associated With Mountain Waves. WMO Tech. Note, Geneva, Switzerland, 31pp.

Jones, D. N., 1972: An Investigation of a Vertically Scanning Infrared Radiometer As a Clear Air Turbulence Warning System. AFCRL-TR-72-0729, Bedford Mass., 101pp.

Keller, J. L., 1981: Prediction and monitoring of clear air turbulence: an evaluation of the applicability of the rawinsonde system. J. Appl. Meteor. 20, 686-692.

Kuhn, P., F. Caracena, and C. M. Gillespie Jr., 1977: Clear air turbulence: detection by infrared observations of water vapor. Science. 196, 1099-1100.

Lee, D. R., R. B. Stull, and W. S. Irvine, 1979: Clear Air Turbulence Forecasting Techniques. AFGWC/TN 79/001, Air Force Global Weather Central, Omaha, Ne, 64pp.

National Weather Service, 1979: Forecasting Handbook No. 1 Facsimile Products. U. S. Department of Commerce, National National Oceanic and Atmospheric Administration, National Weather Service, Washington D. C., 7-18 - 7-28.

Panofsky, H. A., 1949: Objective weather map analysis. J. Meteor., 6, 386-392.

Petersen, R. A., 1986: Detailed three-dimensional analysis using an objective cross-sectional approach. To appear in Mon. Wea. Rev.

Platt, C. M. R., 1981: Detection of clear air turbulence by water vapor emission anomalies: weighting functions and sensitivities., Appl. Optics 20, 2510-2516.

Stearns, L. P., F. Caracena, P. M. Kuhn, and R. L. Kurkowski, 1981: Clear air turbulence: an airborne alert system., Science. 213, 1007-10008.

Tennekes, H. and J. L. Lumley, 1972: A First Course In Turbulence, MIT Press, Cambridge, Mass., 300pp.

Thompson, R. O. R. Y., 1980: Efficiency of conversion of kinetic energy to potential energy by a breaking internal gravity wave, J. Geophys. Res. 85, 6631-6635.

Thorpe, S. A., 1973: Turbulence in stably stratified fluids. Boundary Layer Meteor. 45, 95-119.

U. S. Naval Weather Service, 1976: Numerical Environmental Products Manual. NAVAIR 50-1g-522, U. S. Navy, Washington D. C., 246pp.

Vinnichenko, N. K., N. Z. Pinus, S. M. Shmeter, and G. N. Shur, 1980: Turbulence in the Free Atmosphere. Dolgoprudnyi, USSR (Translated into English by Consultants Bureau), 310pp.

AD-A168 400 CLEAR AIR TURBULENCE ANALYSIS USING ISENTROPIC METHODS 2/2
(U) NAVAL POSTGRADUATE SCHOOL MONTEREY CA J H JACOBSON
MAR 86

UNCLASSIFIED F/G 4/2 NL

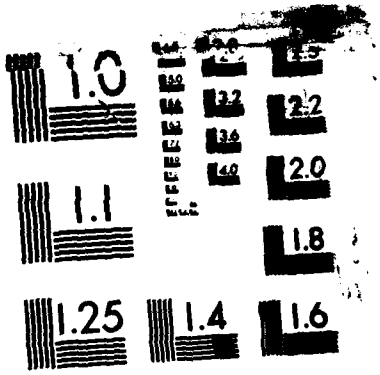

INITIAL DISTRIBUTION LIST

		No. Copies
1.	Defense Technical Information Center Cameron Station Alexandria, VA 22304-6145	2
2.	Library, Code 0142 Naval Postgraduate School Monterey, CA 93943-5002	2
3.	Chairman (Code 63Rd) Department of Meteorology Naval Postgraduate School Monterey, CA 93943-5000	1
4.	Professor C. Wash (Code 63Wa) Department of Meteorology Naval Postgraduate School Monterey, CA 93943-5000	10
5.	Capt John H. Jacobson AFGWC/SDDP Offutt AFB, Ne 68113-5000	1
6.	Director Naval Oceanography Division Naval Obaervatory 34th and Massachusetts Ave NW Washington, DC 20390-5000	1
7.	Commander Naval Oceanography Command NSTL Bay St. Louis, MS 39522-5000	1
8.	Commanding Officer Naval Oceanographic Office NSTL Station Bay St. Louis, MS 39522-5000	1
9.	Commanding Officer Fleet Numerical Oceanographic Office Monterey, Ca 93943-5000	1
10.	Commanding Officer Naval Environmental Prediction Research Facility Monterey, Ca 93943-5006	1

11. Commanding Officer 1
Naval Ocean Research and Development Activity
NSTL Station
Bay St. Louis, MS 39522-5000

12. Chairman, Oceanography Department 1
U. S. Naval Academy
Annapolis, MD 21402-5000

13. Chief of Naval Research 1
800 N. Quincy St.
Arlington, VA 22217-5000

14. Office of Naval Research (Code 420) 1
Naval Ocean Research and Development Activity
800 N. Quincy St.
Arlington, VA 22217-5000

15. AFIT/CISK 1
Wright Patterson AFB, OH 45433-5000

16. AWS/CC 1
Scott AFB, IL 62225-5000

17. AFGWC/CC 1
Offutt AFB, NE 68113-5000

18. AFGWC/WF 1
Offutt AFB, NE 68113-5000

END

DTIC

7-86